

**Black holes and large order quantum geometry**Min-xin Huang,<sup>1</sup> Albrecht Klemm,<sup>1,2</sup> Marcos Mariño,<sup>3</sup> and Alireza Tavanfar<sup>3,4</sup><sup>1</sup>*Department of Physics, University of Wisconsin, Madison, Wisconsin 53706, USA*<sup>2</sup>*Department of Mathematics, University of Wisconsin, Madison, Wisconsin 53706, USA*<sup>3</sup>*Department of Physics, CERN, Geneva 23, CH-1211 Switzerland*<sup>4</sup>*Institute for Studies in Theoretical Physics and Mathematics (IPM), P.O. Box 19395-5531, Tehran, Iran*

(Received 14 December 2008; published 2 March 2009)

We study five-dimensional black holes obtained by compactifying M theory on Calabi-Yau threefolds. Recent progress in solving topological string theory on compact, one-parameter models allows us to test numerically various conjectures about these black holes. We give convincing evidence that a microscopic description based on Gopakumar-Vafa invariants accounts correctly for their macroscopic entropy, and we check that highly nontrivial cancellations—which seem necessary to resolve the so-called entropy enigma in the Ooguri-Strominger-Vafa conjecture—do in fact occur. We also study analytically small 5d black holes obtained by wrapping M2 branes in the fiber of K3 fibrations. By using heterotic/type II duality we obtain exact formulae for the microscopic degeneracies in various geometries, and we compute their asymptotic expansion for large charges.

DOI: [10.1103/PhysRevD.79.066001](https://doi.org/10.1103/PhysRevD.79.066001)

PACS numbers: 11.25.Mj, 04.70.Dy, 11.25.Yb

**I. INTRODUCTION**

String theory can provide in many situations a precise microscopic description of supersymmetric black holes which reproduces for large charges the Bekenstein-Hawking entropy [1]. Degeneracies of microstates that are highly protected by supersymmetry are often counted by mathematically well understood quasitopological quantities related to the compactification manifold. For example, the computation of microstates of the D1-D5 system is encoded in the elliptic genus of a symmetric product of a hyper-Kähler manifold (see [2,3] for a review of these computations).

A very challenging class of black holes in string theory is obtained by compactifying M theory on a Calabi-Yau (CY) manifold  $X$  with generic  $SU(3)$  holonomy. These are five-dimensional black holes, which are characterized by a membrane charge  $Q \in H_2(X, \mathbb{Z})$  and an angular momentum  $m$ . It was proposed in [4] that the microscopic entropy of these black holes is accounted for by BPS states associated to M2 branes wrapping the cycle  $Q$  and with left spin  $m = 2j_L$  in five dimensions. According to the proposal of [4] their degeneracies are encoded in the five-dimensional supersymmetric index

$$I(\alpha, \beta) = \text{Tr}(-1)^{2j_L + 2j_R} \exp(-\alpha j_L - \beta H). \quad (1.1)$$

The information captured by this index can be extracted from the all-genus expansion of the holomorphic free energy of the topological string, computed at the large radius point of  $X$  [5],

$$\lim_{\bar{t} \rightarrow \infty} F(t, \bar{t}, g_s) = \sum_{g=0}^{\infty} g_s^{2g-2} F_g(t). \quad (1.2)$$

In this identification the BPS degeneracies are mapped to the Gromov-Witten invariants of genus  $g$  holomorphic maps. Since the topological string could not be solved on compact Calabi-Yau threefolds at higher genus, progress in understanding the microscopic degeneracies in the general case was very limited. On the boundary of the Kähler cone the problem might reduce effectively to a counting problem on a two complex dimensional surface, which is mathematically simpler, but the situation is also physically more degenerate. When the compactification manifold is  $X = X_2 \times \mathbb{T}^2$ , where  $X_2 = \mathbb{T}^4$  or K3, one obtains the five-dimensional black hole solutions constructed in [6], and the microscopic degeneracies are encoded in the elliptic genus of symmetric products of  $X_2$ .

In this paper we study the microscopic counting proposed in [4] in two different situations, by using numerical and analytic methods. First of all, we consider 5d black holes obtained by compactifying M theory on the one-parameter Calabi-Yau spaces studied in [7]. This explores a generic direction in the Kähler cone and allows to describe generic 5d black holes, which have nonvanishing classical horizon area and can carry spin. In [7] significant progress was made in solving the topological string on compact Calabi-Yau threefolds. By combining the holomorphic anomaly of [8] with modularity properties of the topological string partition function  $Z = \exp(F)$ , effective action arguments, and Castelnuovo theory, it was possible to calculate the topological string free energy up to genus 53.

In order to make contact with black hole physics on the (super)gravity side, one has to obtain the asymptotic expansion of the microscopic degeneracies for large charge  $Q$

\*minxin@physics.wisc.edu

†aklemm@physics.wisc.edu

‡marcos@mail.cern.ch

§alireza.tavanfar@cern.ch

and  $Q \gg m$ . For fixed  $g$  the expansion of  $F_g(t)$  around large radius is convergent and under analytic control by mirror symmetry. In contrast, the genus expansion in (1.2) is expected to be asymptotic, as in noncritical string theories [9] (see [10] for a recent discussion of this issue in the context of topological strings). To obtain a large  $Q$  expansion for the degeneracies of the  $(Q, m)$  states one needs information at genus  $g \sim Q^2$  and is hence facing the issues of the behavior of string theory at large genus. Although we do not have enough control of the degeneracies to obtain analytical results on the large charge expansion, the situation is suited to a numerical study by using the method of Richardson transforms.<sup>1</sup> This method merely relies on the knowledge of the form of the series and makes it possible to extract its coefficients from the value of the degeneracies at finitely many points. The analysis is complicated by the fact that the large charge expansion of the degeneracies is an asymptotic expansion, but we find that the Richardson transforms converge rapidly to the expected macroscopic values for the asymptotic coefficients. To estimate its accuracy we sample over the 13 Calabi-Yau manifolds, which have a sufficiently wide variety of topological data. Using this sample we can conclude that, given our present data of the higher genus instanton expansion, the leading coefficient of the asymptotic expansion is correct within 2% and the first subleading one within 12%. With this information at hand, we give convincing evidence that the topological string accounts correctly for the entropy of 5d spinning black holes, as conjectured in [4].<sup>2</sup>

Some aspects of the genus expansion (1.2) are much better understood in terms of D-brane invariants like Gopakumar-Vafa (GV) or Donaldson-Thomas invariants, rather than Gromov-Witten invariants. In particular, for a given charge  $Q \in H_2(X, \mathbb{Z})$  and  $Q \neq 0$  one gets the complete genus information from a finite number of GV invariants. We use the results for  $F_g$  in [7] to obtain precise information on the Donaldson-Thomas invariants of the one-parameter models. This allows us to study numerically the scaling exponent  $k$  considered in [12] (and defined below in (4.7) and (4.8)), which governs the growth of the Donaldson-Thomas invariants under rescalings of the charges. Our numerical study indicates that  $k = 2$ . As argued in [12], this value indicates that highly nontrivial cancellations occur between the contributions to the Donaldson-Thomas invariants, which in turn seem necessary to resolve the so-called entropy enigma [12] in the Ooguri-Strominger-Vafa (OSV) conjecture [13].

The second class of black holes we study has a different flavor. These are 5d black holes which are obtained when the Calabi-Yau manifold is a K3 fibration and the charge  $Q$  is restricted to the K3 fiber. Their classical horizon area is

zero (i.e. they are small black holes) and have no spin. By using heterotic/type II duality one can obtain analytic formulae for the  $F_g$  amplitudes at all  $g$  [14–18], and from them one can extract the exact microscopic degeneracies for the corresponding small 5d black holes. Of course, as explained, for example, in [12], the most delicate aspects of 5d spinning black holes, as well as of the OSV conjecture, cannot be tested with small black holes. This reflects the fact that the Gromov-Witten theory of K3 fibers (which is closely related to the theory of Hilbert schemes) is much simpler than the Gromov-Witten theory of generic Calabi-Yau manifolds. However, having an exact microscopic counting might be important in understanding some detailed aspects of the entropy. As in the 4d case considered in [19], the 5d degeneracies are closely related to modular forms, but one cannot use the Rademacher expansion featured in [19,20]. We find, however, an exact asymptotic expansion for the microscopic degeneracies in powers of the inverse charge (albeit corrected by terms which are exponentially suppressed for large charges). The leading term of the asymptotics is in agreement with a macroscopic computation using the 4d/5d connection of [21] and the 4d attractor equations for a D6/D2 system.

The organization of this paper is as follows. In Sec. II we review the macroscopic and microscopic computation of the entropy for 5d spinning black holes. In Sec. III we analyze numerically the asymptotic properties of the degeneracies for the Calabi-Yau manifolds studied in [7]. In Sec. IV we study the asymptotic properties of Donaldson-Thomas invariants to address the entropy enigma of [12]. In Sec. V we study small black holes in K3 fibrations and compute their degeneracies as well as the asymptotic expansion. Finally, in Sec. VI we list some conclusions and open problems.

## II. MICROSCOPIC AND MACROSCOPIC COUNTING FOR 5D BLACK HOLES

### A. Macroscopic description

Let us start with the macroscopic description of black hole entropy. We will consider 5d black holes obtained by compactifying M theory on a Calabi-Yau threefold  $X$ , and characterized by a charge  $Q \in H_2(X, \mathbb{Z})$  and  $SU(2)_L \subset SO(4)$  angular momentum  $m$ . We will introduce a basis  $\Sigma^A$  for  $H_2(X, \mathbb{Z})$ , where  $A = 1, \dots, b_2(X)$ , as well as a dual basis  $\eta_A$  for  $H^2(X)$ . With respect to the  $\Sigma^A$  basis, the charge  $Q$  will be given by a set of integers  $Q_A$ . The classical entropy of these black holes, denoted as  $S_0$ , is one quarter of the horizon area

$$S_0 = 2\pi\sqrt{Q^3 - m^2}, \quad (2.1)$$

where  $Q$  is the graviphoton charge of the black hole. This charge is related to the membrane charge  $Q$  by the attractor mechanism in five dimensions [22], which states that

<sup>1</sup>For sub-subleading terms we use the Padé approximation.

<sup>2</sup>For a recent study of this question by using an approach totally different from ours, see [11].

$$\mathcal{Q}^{3/2} = \frac{1}{6} C_{ABC} y^A y^B y^C, \quad (2.2)$$

where

$$\frac{1}{2} C_{ABC} y^B y^C = \mathcal{Q}_A, \quad (2.3)$$

and

$$C_{ABC} = \int_X \eta_A \wedge \eta_B \wedge \eta_C \quad (2.4)$$

are the triple intersection numbers of  $X$ . For one-parameter models, the membrane charge will be identified with the degree  $d$  of the holomorphic map in topological string computations, and we will denote the single intersection number by  $C_{ABC} = \kappa$ . From the above equations it follows that

$$\mathcal{Q} = \left(\frac{2}{9\kappa}\right)^{1/3} d. \quad (2.5)$$

There is a correction to the black hole entropy from the  $R^2$  term of the supergravity effective action, which we denote as  $S_1$  for convenience. The  $R^2$  term correction to the black hole entropy scales like  $\mathcal{Q}^{1/2}$  in the large charge limit, and was computed in [23] by using Wald's formula [24] for the  $R^2$  in 5d. The result reads

$$S_1 = \frac{\pi}{24} \sqrt{Q^3 - m^2} c_2 \cdot Y \left( \frac{3}{Q} + \frac{m^2}{Q^4} \right), \quad (2.6)$$

where

$$Y^A = \frac{1}{Q^{1/2}} y^A \quad (2.7)$$

and

$$c_{2A} = \int_X c_2(X) \wedge \eta_A. \quad (2.8)$$

For  $m = 0$  this formula has been rederived in [25,26] by using the full 5d SUGRA action. In the one-parameter case, this correction reads

$$S_1 = \frac{\pi c_2}{8} \left(\frac{6}{\kappa}\right)^{1/3} \sqrt{Q^3 - m^2} \left(\frac{1}{Q} + \frac{m^2}{3Q^4}\right). \quad (2.9)$$

Besides the corrections that we have considered, there are well-known correction terms in the low energy effective action of the form  $F^{2g-2} R^2$ ,  $g \geq 2$ , where  $F$  is the graviphoton field strength. The leading contribution comes from a classical term, which is the contribution of the constant map from a genus  $g$  world sheet to the Calabi-Yau manifold. It is of the form

$$d_g \chi, \quad (2.10)$$

where  $\chi$  is the Euler number of the Calabi-Yau threefold and

$$d_g = \frac{(-1)^g |B_{2g} B_{2g-2}|}{4g(2g-2)(2g-2)!}. \quad (2.11)$$

We denote the correction to black hole entropy due to the  $F^{2g-2} R^2$  term as  $S_g$ . We can roughly estimate the correction for nonspinning black holes  $m = 0$  as follows.

The graviphoton charge is the integral of its field strength over the horizon of black hole,

$$\mathcal{Q} \sim \int_{\text{horizon}} F. \quad (2.12)$$

Since the area of the horizon scales like  $A \sim \mathcal{Q}^{3/2}$ , the graviphoton field strength goes like

$$F \sim \mathcal{Q}^{-(1/2)}. \quad (2.13)$$

The  $R^2$  term contributes a factor  $\mathcal{Q}^{-1}$  in Wald's formula for the black hole entropy, and taking into account also the factor of horizon area  $A \sim \mathcal{Q}^{3/2}$ , we find the scaling behavior of the  $F^{2g-2} R^2$  term correction to black hole entropy to be

$$S_g \sim \chi \mathcal{Q}^{(3/2)-g}, \quad (2.14)$$

where we have included the Euler number from (2.10). The constant of proportionality in (2.14) is now universal and independent of specific Calabi-Yau geometries and the black hole charge. We will be able to make a rough test of (2.14) for the genus 2 case, which is the sub-subleading correction in the large  $\mathcal{Q}$  limit.

There are other world-sheet instanton corrections to the low energy effective action that can be computed also by topological strings. However, these terms are exponentially small in large charge  $\mathcal{Q}$  limit where the supergravity description is valid, and are much suppressed compared to the  $\mathcal{Q}^{-1}$  power corrections in (2.14). In this paper we will not need to consider these world-sheet instanton corrections in the macroscopic description of the black hole entropy. Interestingly these world-sheet instanton corrections are closely related to the BPS states that we will count in the microscopic description of the black hole entropy.

## B. Microscopic description

Microscopically, a 5d black hole with membrane charge  $Q \in H_2(X, \mathbb{Z})$  is engineered by wrapping M2 branes around the two-cycle  $Q$ . This leads to a supersymmetric spectrum of BPS states in 5d which are labeled by  $Q$  and by their spin content  $(j_L, j_R)$ . As argued in [5], in order to obtain an index one has to trace over  $j_R$  (with an insertion of  $(-1)^{2j_R}$ ). The resulting spectrum for a membrane charge  $Q$  can be represented as

$$R_Q = \sum_{r=0}^g n_Q^r I_{r+1}, \quad (2.15)$$

where

$$I_\ell = \left[ 2(\mathbf{0}) + \left(\frac{\mathbf{1}}{2}\right) \right]^\ell \quad (2.16)$$

encodes the spin content  $j_L$ , and  $n_Q^r$  are the Gopakumar-

Vafa invariants [5]. Notice that in (2.15), the sum over  $r$  is finite and the highest spin  $g$  appearing in the sum depends on the membrane charge  $Q$ . In other words, for any given  $Q$  there are only finitely many  $g$  for which the  $n_Q^r$  are nonzero.

We can now write down a generating function for the supersymmetric degeneracies of BPS states with membrane charge  $Q$ , keeping track of their left spin  $j_L$  by computing

$$\sum_m \Omega(Q, m) = \sum_Q \text{tr}_{R_Q} (-1)^{2j_L} y^{j_L}. \quad (2.17)$$

Using the decomposition (2.15) one finds

$$\Omega(Q, m) = \sum_r \binom{2r+2}{m+r+1} n_Q^r, \quad (2.18)$$

where  $m = 2j_L$ . In [4] it was proposed that this quantity gives the microscopic degeneracies for a spinning 5d black hole of charge  $Q$  and spin  $J = m$ . The computation of these degeneracies reduces then to the computation of the Gopakumar-Vafa invariants  $n_Q^r$ . The most effective way to determine these is by computing the genus  $r$  amplitudes  $F_r$  of topological string theory on  $X$ . As shown in [5], the total free energy

$$F(t, g_s) = \sum_{r=0}^{\infty} F_r(t) g_s^{2r-2} \quad (2.19)$$

can be written in terms of the Gopakumar-Vafa invariants as

$$F(t, g_s) = \sum_{r=0}^{\infty} \sum_{Q \in H_2(X)} \sum_{k=1}^{\infty} n_Q^r \frac{1}{k} \left( 2 \sin \frac{k g_s}{2} \right)^{2r-2} e^{-kQ \cdot t}. \quad (2.20)$$

This means, in particular, that one can obtain the  $n_Q^r$  for all  $Q$  by knowing  $F_0, \dots, F_r$ . The black hole entropy is given by the logarithm of the number of microstates

$$S(Q, m) = \log(\Omega(Q, m)). \quad (2.21)$$

This should agree with the macroscopic result in the large charge limit  $Q \gg 1$  and  $Q \gg m$ .

As explained in [4], this proposal for the microscopic counting of states of 5d black holes can be regarded as a generalization of the elliptic genus, which computes BPS degeneracies of the D1-D5 system. Indeed, if one considers M theory compactified on  $X = \text{K3} \times \mathbb{T}^2$ , the generic M2 brane charge in this compactification is

$$Q = [C] + n[\mathbb{T}^2], \quad n \in \mathbb{Z}, \quad (2.22)$$

and  $C$  is a curve in K3. By standard dualities this system can be related to type IIB on  $\text{K3} \times \mathbb{S}^1$  with D-brane charge  $[C]$  and  $M$  units of momentum around  $\mathbb{S}^1$ , which is a close cousin of the D1-D5 system. As it is well known (see, for example, [3]), the BPS degeneracies of this system can be

computed from the elliptic genus of the symmetric product of K3. Let

$$\chi(\text{K3}; q, y) = \sum_{m, \ell} c(m, \ell) q^m y^\ell \quad (2.23)$$

be the elliptic genus of K3. The generating function of elliptic genera of the symmetric product  $S^k \text{K3}$

$$\begin{aligned} \chi(S_p \text{K3}; q, y) &= \sum_{k=0}^p \chi(S^k \text{K3}; q, y) p^k \\ &= \sum_{k, n, m} c(k, n, m) p^k q^n y^m \end{aligned} \quad (2.24)$$

can be computed from the coefficients in (2.23) in terms of an infinite product [27]

$$\chi(S_p \text{K3}; q, y) = \prod_{N, M \geq 0, \ell} (1 - p^N q^M y^\ell)^{-c(NM, \ell)}. \quad (2.25)$$

The supersymmetric degeneracies of BPS states for this system are then given by the coefficients of the expansion in (2.24),

$$\Omega(Q, m) = c\left(\frac{1}{2}C^2 + 1, n, m\right), \quad (2.26)$$

where  $Q$  is of the form (2.22). One can show that, for large charges [3,28],

$$\log \Omega(Q, m) \sim 2\pi \sqrt{\frac{n}{2} C^2 - m^2}. \quad (2.27)$$

It is easy to check that this is precisely the macroscopic entropy (2.1) computed for  $\text{K3} \times \mathbb{T}^2$ . Of course, the degeneracies (2.18) are in general much more difficult to compute, since they correspond to black holes with only  $\mathcal{N} = 1$  supersymmetry in 5d.

### III. ONE-PARAMETER MODELS

#### A. Topological strings on one-parameter models

In [7] the topological B model was integrated on 13 one-parameter Calabi-Yau spaces which can be realized as hypersurfaces or complete intersections in (weighted) projective spaces. We have listed these spaces and some of their topological data in Table I. These data are the intersection numbers  $C_{ABC} = \kappa$ , the second Chern classes  $c_2$ , and the Euler numbers  $\chi$ . They are needed for computations of the macroscopic entropy.

The complex moduli space of these threefolds is  $\mathcal{M} = \mathbb{P}^1 \setminus \{\infty, 1, 0\}$ , and the three special points are the large radius degeneration point, a conifold point, and a further point either of finite (Gepner point) or infinite branching order. The modular group  $\Gamma_X \in \text{SP}(4, \mathbb{Z})$  can hence be generated e.g. by the large radius and the conifold monodromies.

The conceptual obstacle in integrating the B-model holomorphic anomaly [8] is the holomorphic ambiguity which arises in each integration step. Invariance of the

TABLE I. The sample of 13 one-parameter complete intersection CY models in weighted projective spaces. A complete intersection Calabi-Yau of degree  $d_1, \dots, d_k$  in weighted projective space  $\mathbb{P}^{l-1}(w_1, \dots, w_l)$  is denoted  $X_{d_1, \dots, d_k}(w_1, \dots, w_l)$ , i.e. weights  $w$  with repetition  $m$  are abbreviated by  $w^m$ .  $\chi = \int_X c_3$  is the Euler number,  $\kappa$  is the triple intersection number, and  $c_2 \cdot \eta$  is defined in (2.8).

| CY model                 | $\chi$ | $c_2 \cdot \eta$ | $\kappa$ | CY                     | $\chi$ | $c_2 \cdot \omega$ | $\kappa$ |
|--------------------------|--------|------------------|----------|------------------------|--------|--------------------|----------|
| $X_5(1^5)$               | -200   | 50               | 5        | $X_6(1^4, 2)$          | -204   | 42                 | 3        |
| $X_8(1^4, 4)$            | -296   | 44               | 2        | $X_{10}(1^3, 2, 5)$    | -288   | 34                 | 1        |
| $X_{3,3}(1^6)$           | -144   | 54               | 9        | $X_{4,2}(1^6)$         | -176   | 56                 | 8        |
| $X_{3,2,2}(1^7)$         | -144   | 60               | 12       | $X_{2,2,2,2}(1^8)$     | -128   | 64                 | 16       |
| $X_{4,3}(1^5, 2)$        | -156   | 48               | 6        | $X_{4,4}(1^4, 2^2)$    | -144   | 40                 | 4        |
| $X_{6,2}(1^5, 3)$        | -256   | 52               | 4        | $X_{6,4}(1^3, 2^2, 3)$ | -156   | 32                 | 2        |
| $X_{6,6}(1^2, 2^2, 3^2)$ | -120   | 32               | 1        |                        |        |                    |          |

topological string amplitudes under  $\Gamma_X$  and effective action arguments, which govern the behavior of the genus  $g$  amplitudes at special points, restrict the ambiguity to  $3g - 3$  unknowns [4]. By using a refined effective action analysis, which gives rise to the ‘‘gap condition’’ at the conifold, regularity at the orbifold, and Castelnuovo’s bound for the Gromow-Witten invariants at large radius, it is possible to fix the unknowns, and one can calculate the free energy of the topological string to arbitrary degree and up to genus 12–53.

Instead of using the generic solution of holomorphic anomaly equation suggested by the world-sheet degenerations [8] we use the constraints of  $\Gamma_X$  on the topological string amplitudes directly when integrating the holomorphic anomaly equations genus by genus [29,30]. This results in an algorithm, which constructs the genus  $g$  amplitudes as weight  $3g - 3$  polynomials over a ring of three anholomorphic and one holomorphic modular objects of weight (1, 2, 3, 1). As a consequence the number of terms in the  $F_g$  grows polynomial with  $g$  and not exponentially as in the approach of [8].<sup>3</sup>

The approach of [7] views the topological string partition function as a wave function over  $H^3(X, \mathbb{R})$ . Choices of polarization are necessary in order to expand the effective action at different points in the moduli space  $\mathcal{M}$ , in appropriate local holomorphic coordinates. Most of the black hole issues that we will discuss involve the degeneracies extracted from the topological string at the large radius limit. Therefore we will discard for now most of the global information and focus only the holomorphic limit of the topological string partition function at this limit, where it encodes the degeneracy of bound states of a single D6 brane and arbitrary D2-D0 branes.

## B. Static black holes

We first consider the case of nonspinning black hole  $J \equiv m = 0$  and denote  $N_d = \Omega(d, 0)$ . The entropy formula

<sup>3</sup>Nevertheless the limiting factor in advancing to higher  $g$  is presently not the ambiguity but the computing time. The reason is that the numerators in the coefficients of the polynomials grow exponentially.

including the first few orders (2.1), (2.9), and (2.14) is in this case

$$S = b_0 d^{3/2} + b_1 d^{1/2} + \frac{b_2}{d^{1/2}} + \mathcal{O}\left(\frac{1}{d^{3/2}}\right), \quad (3.1)$$

where the first two coefficients are

$$b_0 = \frac{4\pi}{3\sqrt{2\kappa}}, \quad b_1 = \frac{\pi c_2}{4\sqrt{2\kappa}}, \quad (3.2)$$

and we have used the graviphoton charge relation (2.5). The coefficient  $b_1$  of the subleading term is consistent with the results in [25,26,31], where it was observed that the  $b_1$  can be produced by a shift of the 2-brane charge

$$d \rightarrow d + \frac{c_2}{8} \quad (3.3)$$

in the leading term.

To compare with the microscopic counting we define the following function:

$$f(d) = \frac{\log(N_d)}{d^{3/2}}. \quad (3.4)$$

The macroscopic black hole entropy predicts that the large order behavior of  $f(d)$  is

$$f(d) = b_0 + \frac{b_1}{d} + \frac{b_2}{d^2} + \dots \quad (3.5)$$

Since we have available only the values of  $f(d)$  for positive integer  $d$  up to a finite degree, it is appropriate to use well-known numerical methods to extrapolate the asymptotic value  $b_0$ . From the form of the subleading corrections in (3.5), it is appropriate to use the Richardson extrapolation method (see, for example, [32]).

The basic idea of this numerical method is simple. To cancel the subleading corrections in (3.5) up to order  $1/d^N$ , one defines

$$A(d, N) = \sum_{k=0}^N \frac{f(d+k)(d+k)^N (-1)^{k+N}}{k!(N-k)!}. \quad (3.6)$$

One can show that if the perturbation series (3.5) truncates at order  $1/d^N$ , the expression (3.6) will give exactly the

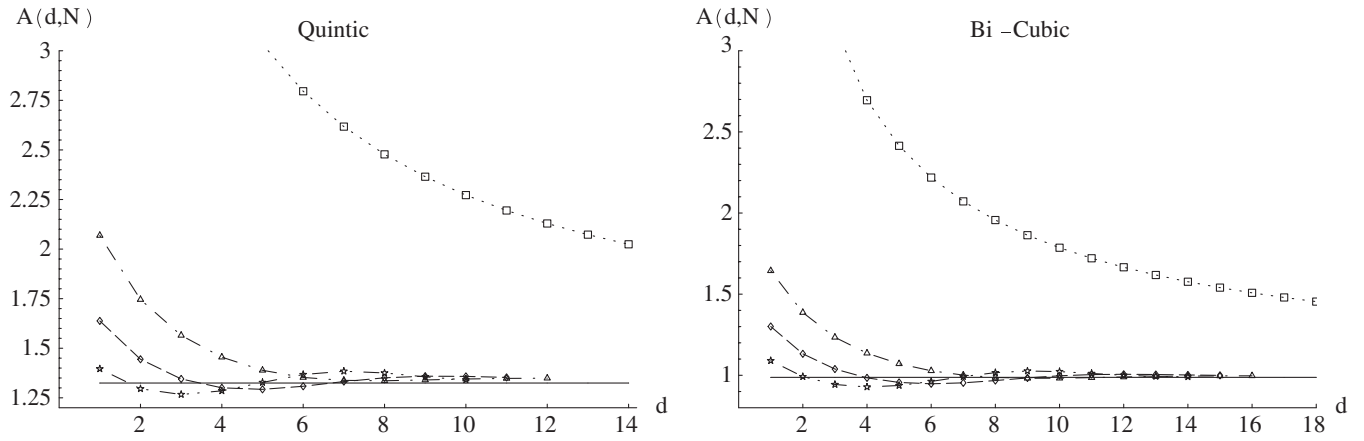


FIG. 1. Microscopic data for  $f(d)$  ( $\square$ ), and the Richardson transforms  $A(d, 2)$  ( $\triangle$ ),  $A(d, 3)$  ( $\diamond$ ), and  $A(d, 4)$  ( $\star$ ). The straight line corresponds to the macroscopic prediction  $b_0 = \frac{4\pi}{3\sqrt{2\kappa}}$ . For the quintic this value is  $b_0 \approx 1.359$  and for the available degree 14 the Richardson transforms lie 1.8%, 2.1%, 1.2% from the macroscopic prediction. For the bicubic  $b_0 \approx 0.967$ , the available degree is higher, 18, and the microscopic counting is within 0.9%, 1.2%, 0.3% from the macroscopic prediction. As an example we give BPS numbers used for the analysis at degree 18 of the bicubic in Table VII.

asymptotic value  $b_0$ . Ideally, the larger  $N$  and  $d$  are, the closer  $A(d, N)$  is to the asymptotic value. But due to the limitation of our data, the sum  $d + N$  must not exceed the maximal degree  $d_{\max}$  of the topological string computations.

Figure 1 shows the convergence of the leading terms in  $f(d)$  and of the Richardson transforms  $A(d, N)$ ,  $N = 2, 3, 4$  for the quintic and the bicubic. It is obvious from the two examples in Fig. 1 that the Richardson method improves impressively the convergence of the series, i.e. it provides a model independent and consistent scheme to suppress the subleading corrections. Using  $N = 2-4$  is good enough for our purpose of estimating the asymptotic value. We conduct the analysis for all 13 models using  $N = 3$  and the maximal degree available. The results are summarized in Table II and are in very good agreement with the expected asymptotic values  $b_0$  in (3.2). More detailed results on all

the analysis carried out in this paper can be found in a script and in a database at [30].

We can further extract the subleading coefficient  $b_1$  from the data. Define

$$f_1(d) = (f(d) - b_0)d,$$

$$A_1(d, N) = \sum_{k=0}^N \frac{f_1(d+k)(d+k)^N (-1)^{k+N}}{k!(N-k)!}, \quad (3.7)$$

and the asymptotic value of  $f_1(d)$  should be  $b_1$ . We apply the same Richardson extrapolation method to  $f_1(d)$  and we compare it with the macroscopic black hole predictions. Two typical examples for the behavior of the Richardson transforms are plotted in Fig. 2. The results for all models are summarized in Table III.

TABLE II. Comparing the extrapolated value of  $b_0$  with the macroscopic prediction.

| Calabi-Yau model         | $d_{\max}$ | $A(d_{\max} - 3, 3)$ | $b_0 = \frac{4\pi}{3\sqrt{2\kappa}}$ | Error  |
|--------------------------|------------|----------------------|--------------------------------------|--------|
| $X_5(1^5)$               | 14         | 1.353 06             | 1.324 61                             | 2.15%  |
| $X_6(1^4, 2)$            | 10         | 1.755 59             | 1.710 07                             | 2.66%  |
| $X_8(1^4, 4)$            | 7          | 2.114 54             | 2.0944                               | 0.96%  |
| $X_{10}(1^3, 2, 5)$      | 5          | 2.992 11             | 2.961 92                             | 1.02%  |
| $X_{3,3}(1^6)$           | 17         | 1.002 04             | 0.987 307                            | 1.49%  |
| $X_{4,2}(1^6)$           | 15         | 1.070 31             | 1.0472                               | 2.21%  |
| $X_{3,2,2}(1^7)$         | 10         | 0.821 169            | 0.855 033                            | -3.96% |
| $X_{2,2,2,2}(1^8)$       | 13         | 0.722 466            | 0.740 48                             | -2.43% |
| $X_{4,3}(1^5, 2)$        | 11         | 1.216 26             | 1.2092                               | 0.58%  |
| $X_{6,2}(1^5, 3)$        | 11         | 1.527 85             | 1.480 96                             | 3.17%  |
| $X_{4,4}(1^4, 2^2)$      | 7          | 1.424 01             | 1.480 96                             | -3.85% |
| $X_{6,4}(1^3, 2^2, 3)$   | 5          | 2.068 99             | 2.0944                               | -1.21% |
| $X_{6,6}(1^2, 2^2, 3^2)$ | 4          | 2.950 82             | 2.961 92                             | -0.37% |

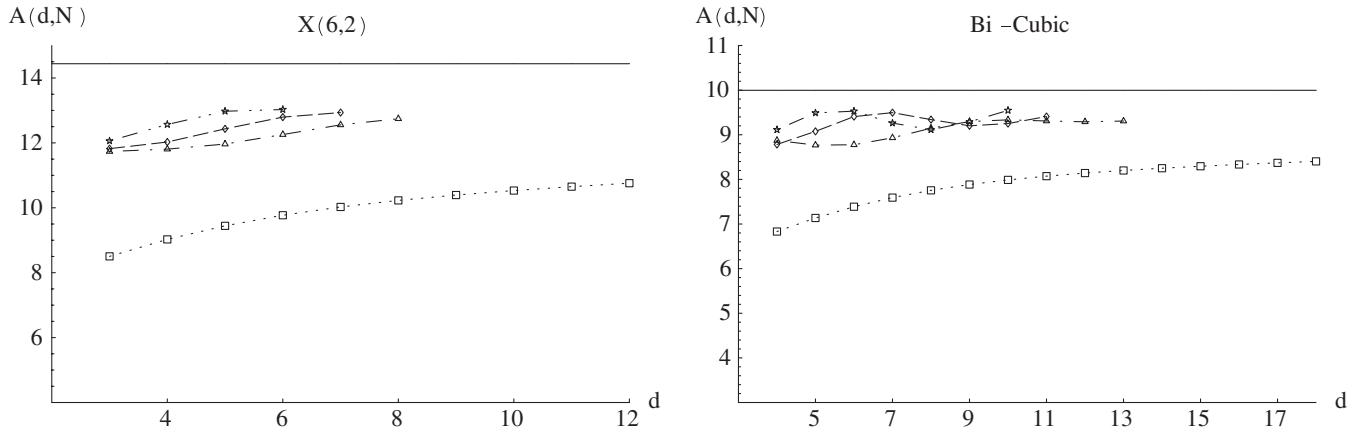


FIG. 2. Microscopic data for  $f(d)$  ( $\square$ ), and the Richardson transforms  $A(d, 4)$  ( $\triangle$ ),  $A(d, 5)$  ( $\diamond$ ), and  $A(d, 6)$  ( $\star$ ). The straight line corresponds to the macroscopic prediction  $b_1 = \frac{\pi c_2}{4\sqrt{2\kappa}}$ . For the degree  $X_{6,2}$  complete intersection this value is  $b_1 \approx 14.44$  and for the available degree 12 the Richardson transforms lie  $-11.7\%$ ,  $-10.4\%$ ,  $-9.77\%$  below the macroscopic prediction. For the bicubic  $b_1 \approx 9.994$ , the available degree is 18 and the microscopic counting is  $-7.15\%$ ,  $-6.88\%$ ,  $-6.63\%$  below the macroscopic prediction.

Despite our rather successful verifications of the numerical coefficients  $b_0$  and  $b_1$ , we should note that the expansion in inverse powers of the charge (3.5) is actually an asymptotic series. The asymptotic character of the large charge expansions of microscopic degeneracies is manifest in the explicit computations for small black holes in [19] and also in the examples we will discuss in Sec. V. In our case, we can relate the asymptotic expansion of (3.5) to a large genus behavior in a string series, since the coefficients in (3.5) are proportional to the constant map contribution

$$b_g \sim d_g, \tag{3.8}$$

where  $d_g$  is given in (2.11). This coefficient grows at large  $g$  as

$$d_g \sim (2\pi)^{-4g} (-1)^g (2g)!, \tag{3.9}$$

which is the typical behavior found in string perturbation

theory [9]. It then follows that the series expansion (3.5) for  $f(d)$  has zero radius of convergence for any value of  $d$  and it is rather an asymptotic expansion. Indeed, the  $d_g$  are the coefficients of the asymptotic expansion of the MacMahon function (see [19], Appendix E, for a detailed derivation). For these kinds of expansions, the best approximation to their true value (which in this case is the function  $f(d)$  computed from topological strings) is obtained by truncating the sum at the order  $\mathcal{N}$  which minimizes the error. For an asymptotic series of the form

$$f(w) = \sum_{k=1}^{\infty} b_k w^k, \quad b_k \sim A^{-k} (\beta k)! \tag{3.10}$$

the optimal truncation occurs generically at

$$\mathcal{N} \sim \frac{1}{\beta} \left( \frac{A}{|w|} \right)^{1/\beta}. \tag{3.11}$$

In our case  $\beta = 2$  and we can estimate  $\mathcal{N}$  as follows.

TABLE III. Comparing the extrapolated value with the macroscopic prediction of  $b_1$ .

| Calabi-Yau model         | $d_{\max}$ | $A_1(d_{\max} - 3, 3)$ | $b_1 = \frac{\pi c_2}{4\sqrt{2\kappa}}$ | Error  | Estimated $b_2$ |
|--------------------------|------------|------------------------|---|--------|-----------------|
| $X_5(1^5)$               | 14         | 11.2668                | 12.4182                                 | -9.27% | -11.9503        |
| $X_6(1^4, 2)$            | 10         | 11.9237                | 13.4668                                 | -11.5% | -12.1848        |
| $X_8(1^4, 4)$            | 7          | 14.0537                | 17.2788                                 | -18.7% | -14.9973        |
| $X_{10}(1^3, 2, 5)$      | 5          | 15.2509                | 18.8823                                 | -19.2% | -14.9817        |
| $X_{3,3}(1^6)$           | 17         | 9.29062                | 9.99649                                 | -7.06% | -9.63958        |
| $X_{4,2}(1^6)$           | 15         | 10.0226                | 10.9956                                 | -8.85% | -10.7834        |
| $X_{3,2,2}(1^7)$         | 10         | 8.45163                | 9.61912                                 | -12.1% | -9.3828         |
| $X_{2,2,2,2}(1^8)$       | 13         | 7.84595                | 8.88577                                 | -11.7% | -8.88773        |
| $X_{4,3}(1^5, 2)$        | 11         | 9.5981                 | 10.8828                                 | -11.8% | -9.96404        |
| $X_{6,2}(1^5, 3)$        | 11         | 12.5614                | 14.4394                                 | -13.0% | -14.2582        |
| $X_{4,4}(1^4, 2^2)$      | 7          | 9.70091                | 11.1072                                 | -12.7% | -9.41295        |
| $X_{6,4}(1^3, 2^2, 3)$   | 5          | 11.1008                | 12.5664                                 | -11.7% | -10.0821        |
| $X_{6,6}(1^1, 2^2, 3^3)$ | 4          | 11.1378                | 12.2179                                 | -8.84% | -8.15739        |

According to the connection between 4D/5D black holes [21], the attractor value for the topological string coupling constant is  $g_s = 4\pi$  [23]. This should be roughly the numerical constant that relates the graviphoton field strength to the charge  $Q$  in (2.13), and it contributes to the coefficients  $b_g$  an extra factor  $g_s^{2g-2}$ , so that we can refine (3.8) to

$$b_g \sim (4\pi)^{2g} d_g, \quad (3.12)$$

and the constant in (3.10) is  $A = \pi^2$ . Therefore, the optimal truncation is at

$$\mathcal{N} \sim \frac{\pi}{2} d^{1/2}. \quad (3.13)$$

For the small values of  $d$  that we are considering we should therefore expect an optimal truncation around  $\mathcal{N} \sim 5-10$ .

These considerations have implications for our numerical analysis. The Richardson method (3.6) is designed in principle for convergent expansions. For asymptotic expansions, we should expect it to give increasing precision and convergence to the true coefficients as long as the order of the transformation  $N$  in (3.6) is lower than the truncation order  $\mathcal{N}$ . This is the underlying reason that prevents us from improving the precision of the leading coefficients by simply increasing the truncation order  $N$  in the Richardson method, and we indeed find an oscillating behavior around the expected true value for the Richardson transforms with  $N > 5$ .

We try to go one step further and give a rough estimation of the coefficient  $b_2$  in (3.1), which has not been studied in the literature from the supergravity point of view. It turns out that the naive method we use for computing the subleading coefficient  $b_1$  gives too big an estimate, which might be a result that the optimal truncation scheme is no longer a good approximation at this order. In order to improve this, we use the Padé approximation which is well known for summing a divergent series. Given an asymptotic series

$$f(z) = \sum_{i=0}^{\infty} b_i z^i, \quad (3.14)$$

one can evaluate the asymptotic value by defining the following Padé approximation:

$$P_M^N(z) = \frac{\sum_{i=0}^N A_i z^i}{1 + \sum_{i=1}^M B_i z^i}, \quad (3.15)$$

where the coefficients  $A_i$  and  $B_i$  are fixed by Taylor expanding the above Eq. (3.15) around  $z = 0$  and match to the first  $M + N + 1$  terms of the original series (3.14).

We take the theoretical values of  $b_0$  and  $b_1$  from (3.2) and use the Monte Carlo method to randomly generate the subleading coefficients  $b_2, b_3, \dots$ , then use the Padé approximation to evaluate the asymptotic series (3.14) for  $z = \frac{1}{d}$ , where  $d = 1, 2, \dots, d_{\max}$ . We pick the subleading coefficients  $b_i$  ( $i \geq 2$ ) that minimize the difference of the

Padé evaluation with the expected value  $f(d)$  from topological strings, i.e. we minimize

$$\sum_{d=1}^{d_{\max}} \left( \frac{P_M^N(\frac{1}{d})}{f(d)} - 1 \right)^2. \quad (3.16)$$

We find different values of  $N, M$  in the Padé approximation give qualitatively similar results. In the last column in Table III, we give the estimated values of the subleading coefficient  $b_2$  using the scheme  $N = 2, M = 1$ .

Assuming the constant map contribution is the most significant contribution at this order in  $Q$ , the coefficient  $b_2$  should behave like

$$b_2 \sim \chi \kappa^{1/6}. \quad (3.17)$$

We can verify the relation (3.17) by plotting  $b_2$  against the Euler number  $\chi \kappa^{1/6}$  for the 13 Calabi-Yau models we studied. We find as the best-fit coefficient

$$b_2 = 0.047 \chi \kappa^{1/6}, \quad (3.18)$$

see the plot in Fig. 3, which is reasonably consistent with the expectation (3.17).

Using Eq. (2.11) at  $g = 2$ , we can find the numerical values of the genus two constant map contribution  $b_2 \sim 0.00017 g_s^2 \chi \kappa^{1/6}$ . Taking into account that  $g_s \sim \mathcal{O}(10)$ , this is the same order of magnitude as our estimate value of 0.047 from microscopic topological string computation.

### C. Spinning black holes

We can try to extract the spin dependence of the black hole entropy from (2.1). Assuming  $Q \gg J$ , and expanding in  $J/Q$ , we find the following macroscopic prediction for the topological string data,

$$g_m(d) \equiv \frac{d^{3/2}}{m^2} \log \left( \frac{\Omega(d, 0)}{\Omega(d, m)} \right) = p_0 + \mathcal{O}\left(\frac{1}{d}\right), \quad (3.19)$$

where

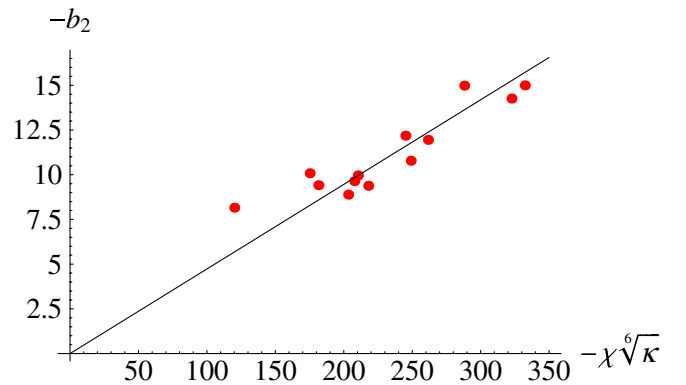


FIG. 3 (color online). The plot of  $-b_2$  vs  $(-\chi \kappa^{1/6})$  for 13 Calabi-Yau models.



TABLE IV. The Richardson method for the quintic with spin  $m = 1, 2, 3$ .

| $d$ | $g_1(d)$  | $A_1(d, 1)$ | $g_2(d)$ | $A_2(d, 1)$ | $g_3(d)$ | $A_3(d, 1)$ |
|-----|-----------|-------------|----------|-------------|----------|-------------|
| 1   | 0.693 147 | 3.227 89    | NA       | NA          | NA       | NA          |
| 2   | 1.960 52  | 6.854 32    | NA       | NA          | NA       | NA          |
| 3   | 3.591 78  | 10.9389     | 9.033 47 | 12.2117     | NA       | NA          |
| 4   | 5.428 56  | 14.4696     | 9.828 04 | 13.0403     | 12.1257  | 6.553 34    |
| 5   | 7.236 77  | 16.4156     | 10.4705  | 12.8183     | 11.0112  | 10.2148     |
| 6   | 8.766 58  | 16.1819     | 10.8618  | 11.6135     | 10.8785  | 9.989 96    |
| 7   | 9.825 91  | 13.9173     | 10.9692  | 9.712 39    | 10.7516  | 8.813 57    |
| 8   | 10.3373   | 10.4832     | 10.8121  | 7.532 59    | 10.5093  | 7.270 17    |
| 9   | 10.3535   | 7.028 69    | 10.4477  | 5.51774     | 10.1494  | 5.736 28    |
| 10  | 10.021    | 4.419 12    | 9.9547   | 3.9872      | 9.708 09 | 4.469 46    |
| 11  | 9.511 78  | 2.9195      | 9.4122   | 3.041 28    | 9.231 85 | 3.583 35    |
| 12  | 8.962 42  | NA          | 8.881 29 | NA          | 8.761 14 | NA          |

$$p_0 = 3\pi\left(\frac{\kappa}{2}\right)^{1/2}. \tag{3.20}$$

For a fixed value  $m$  we use again the Richardson extrapolation method to find the asymptotic value of  $g_m(d)$  for large  $d$ . We list the values of  $g_m(d)$  and its first Richardson extrapolation  $A_m(d, 1)$  for spin  $m = 1, 2, 3$ , using the quintic as an example.

We note that the contribution to entropy from angular momentum is proportional to  $d^{-3/2}$ , as compared to the leading static contribution (3.1) of order  $d^{3/2}$ . Although the prediction (3.19) should be the leading spinning contribution, there could be some small statistical fluctuation of topological string data which is random for the different spins, and which might become comparable to the spinning contribution in (3.19) and result in the deviation for large degree  $d$ . This can be seen in the quintic example in Table IV. We find that the Richardson series does not converge to an asymptotic value, instead the series approach a maximal value before deviating again for large degree  $d$ . In order to minimize the effect of statistical fluctuation of topological string data, we propose to use

the extremal values in the Richardson series  $A_m(d, 1)$  to estimate the asymptotic value of  $p_0$ . This is indeed a relatively good estimate for the quintic case where  $p_0 = 14.9019$ . Other Calabi-Yau manifolds are analyzed in [30].

We analyze the 13 Calabi-Yau models using the above approach. Let us define the extremal value of the first Richardson extrapolation over the degree  $d$  as

$$\tilde{g}_m = A_m(d, 1)|_{\max}. \tag{3.21}$$

For various Calabi-Yau models and spin  $m = 1, 2, 3$ , we compare the value of  $\tilde{g}_m$  with the expected coefficient  $p_0$  given in (3.20). The results are summarized in Table V. We see that for larger angular momentum  $m$  the deviations become bigger, as expected.

#### IV. ASYMPTOTICS OF THE DONALDSON-THOMAS INVARIANTS

As we already mentioned, the total free energy of the topological string (2.19) can be reorganized in terms of Gopakumar-Vafa invariants as in (2.20). A remarkable property of (2.20) is that for a given class  $Q \in H_2(X, \mathbb{Z})$ ,

TABLE V. The Richardson method for the 13 Calabi-Yau models with spin  $m = 1, 2, 3$ .

| Calabi-Yau model         | $p_0 = 3\pi(\frac{\kappa}{2})^{1/2}$ | $\tilde{g}_1$ | $\tilde{g}_1$ error | $\tilde{g}_2$ | $\tilde{g}_2$ error | $\tilde{g}_3$ | $\tilde{g}_3$ error |
|--------------------------|--------------------------------------|---------------|---------------------|---------------|---------------------|---------------|---------------------|
| $X_5(1)$                 | 14.9019                              | 16.4156       | 10.2%               | 13.0403       | -12.5%              | 10.2148       | -31.5%              |
| $X_6(1^4, 2)$            | 11.5429                              | 12.1492       | 5.25%               | 10.1828       | -11.8%              | 8.210 85      | -28.9%              |
| $X_8(1^4, 4)$            | 9.424 78                             | 10.4854       | 11.3%               | 8.1382        | -13.7%              | 5.3473        | -43.3%              |
| $X_{10}(1^3, 2, 5)$      | 6.664 32                             | 6.774 36      | 1.65%               | 5.892 01      | -11.6%              | 3.624 39      | -45.6%              |
| $X_{3,3}(1^6)$           | 19.993                               | 22.1786       | 10.9%               | 17.7804       | -11.1%              | 14.8114       | -25.9%              |
| $X_{4,2}(1^6)$           | 18.8496                              | 21.0741       | 11.8%               | 16.569        | -12.1%              | 12.9935       | -31.1%              |
| $X_{3,2,2}(1^7)$         | 23.0859                              | 25.9065       | 12.2%               | 20.4996       | -11.2%              | 16.5636       | -28.3%              |
| $X_{2,2,2,2}(1^8)$       | 26.6573                              | 30.1999       | 13.3%               | 23.6923       | -11.1%              | 19.2311       | -27.9%              |
| $X_{4,3}(1^5, 2)$        | 16.3242                              | 17.7685       | 8.85%               | 14.4772       | -11.3%              | 12.2514       | -24.9%              |
| $X_{6,2}(1^5, 3)$        | 13.3286                              | 15.2332       | 14.3%               | 11.2819       | -15.4%              | 8.068 44      | -39.5%              |
| $X_{4,4}(1^4, 2^2)$      | 13.3286                              | 13.9081       | 4.35%               | 11.618        | -12.8%              | 10.6901       | -19.8%              |
| $X_{6,4}(1^3, 2^2, 3)$   | 9.42478                              | 9.026 11      | -4.23%              | 7.87731       | -16.4%              | 7.568 62      | -19.7%              |
| $X_{6,6}(1^2, 2^2, 3^2)$ | 6.66432                              | 5.423 33      | -18.6%              | 4.913 55      | -26.3%              | 4.5984        | -31.0%              |

the expression is exact in the string coupling. This is because Castelnuovo's theorem for the ambient space yields  $n_d^g = 0$  for  $d > \alpha\sqrt{g}$  for certain  $\alpha$ .

For example, for the quintic the maximal genus  $g_{\max}$  such that  $n_Q^{g_{\max}} \neq 0$  fulfills a bound

$$g_{\max} \leq \frac{1}{10}(10 + 5d + d^2) \quad (4.1)$$

with a decreasing relative deviation in the large  $d$  limit. The bound is saturated for curves of total degree  $5m$  which are complete intersections of degree  $(1, 5, m)$  in  $\mathbb{P}^4$ , which are smooth curves in the quintic. For  $5 > m > 1$  we can describe the moduli space of the D2 brane as follows. The linear constraint has as a parameter space  $\mathbb{P}^4$  and allows to eliminate one variable from the degree  $m$  constraint, which has as many homogeneous parameters as monomials in four variables, i.e. as many as there are integer solutions to  $\sum_{i=1}^4 n_i = m$ , namely

$$\binom{m+4-1}{m}.$$

The moduli spaces of the curves are therefore fibrations of

$$\mathbb{P}^{\binom{m+4-1}{m}-1}$$

over  $\mathbb{P}^4$ . Using the results of [4] we get for the GV invariant

$$n_{5m}^{g_{\max}} = (-1)^{\binom{m+4-1}{m}-1} \cdot 5 \cdot \binom{m+4-1}{m}. \quad (4.2)$$

If the bound (4.1) is not saturated for small  $d$  the relative deviation can become somewhat larger as seen in Fig. 4.

Let us denote by  $F'(\lambda, t)$  the total free energy without the contribution (2.10). After exponentiation one finds [16]

$$Z'_{\text{GV}}(X, q, t) = \prod_{d=1}^{\infty} \left[ \left( \prod_{r=1}^{\infty} (1 - q^r e^{-dt})^{m_d^0} \right) \times \prod_{g=1}^{\infty} \prod_{l=0}^{2g-2} (1 - q^{g-l-1} e^{-dt})^{(-1)^{g+l} \binom{2g-2}{l} n_d^g} \right], \quad (4.3)$$

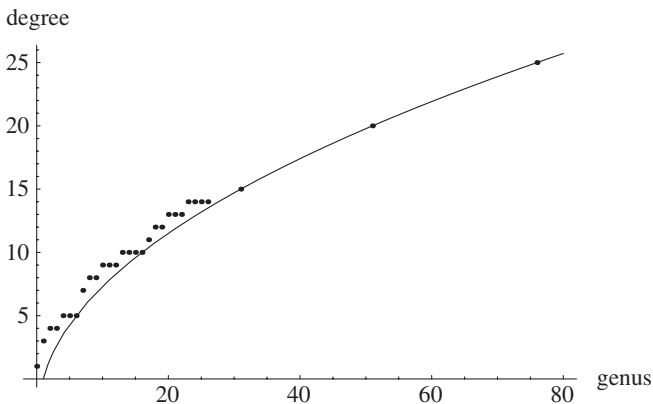


FIG. 4. Castelnuovo's bound for higher genus curves on the quintic. The dots represent  $n_d^{g_{\max}}$  and the curve is (4.1).

where

$$q = e^{i\lambda} \quad (4.4)$$

and we have assumed that there is only one Kähler parameter, so that  $Q$  is labeled by a single integer  $d$ . On the other hand, the conjecture of [33] relating the Donaldson-Thomas invariants  $D_{d,n}$  to Gromov-Witten invariants leads to

$$Z_{\text{DT}}(q, t) = \sum_{d,n} D_{d,n} q^n e^{-dt} = Z'_{\text{GV}}(-q, t) M(-q)^{\chi(X)}, \quad (4.5)$$

where

$$M(q) = \prod_{n=1}^{\infty} \frac{1}{(1 - q^n)^n} \quad (4.6)$$

is the MacMahon function. This term reinstalls the constant map contribution. We list for reference a few Donaldson-Thomas invariants  $D_{d,n}$  on the quintic in Table VI.

After an extensive discussion of possible tests of the OSV conjecture [13], the authors of [12] isolate as a crucial question for the validity of the latter the growth behavior of the Donaldson-Thomas invariants. This behavior is encoded in the scaling exponent  $k$ , defined as

$$\log(D_{\lambda^2 d, \lambda^3 n}) \sim \lambda^k. \quad (4.7)$$

The question is relevant in the range  $d^3 - n^2 > 0$  for which stable black hole configurations exist.

Because of Castelnuovo's bound, and since our data are up to genus 31, we can calculate the Donaldson-Thomas invariants exactly in the range  $0 \leq d \leq 15$  and for arbitrary high  $n$  for the quintic. We are interested in the limit

$$k = \lim_{\lambda \rightarrow \infty} \frac{\log \log |D_{\lambda^2 d, \lambda^3 n}|}{\log \lambda}. \quad (4.8)$$

In order to evaluate it for given values  $(d, n)$  we chose  $\lambda$  so that  $d + l = \lambda^2 d$  for  $d, l \in \mathbb{N}$  and use the fact that  $\log |D_{d+l, n}|$  for fixed  $d, k$  scales in good approximation linearly with  $n$  to calculate the interpolated value of the  $D_{d+l, n'}$  at  $n' = \lambda^3(d, l)n$ , with  $\lambda(d, l) = \sqrt{\frac{d+l}{d}}$ . For  $(d, 0)$  the latter interpolation is of course completely irrelevant and for charges for which the  $n'$  values become large it is not very relevant.

The leading correction to (4.8) is of order  $1/(\log(\lambda))$ . It therefore makes sense to eliminate this leading correction by logarithmic Richardson-Thomas transforms. We define

$$k_l^{(0)} = \frac{\log \log |D_{\lambda(d, l)^2 d, \lambda(d, l)^3 n}|}{\log \lambda(d, l)}, \quad (4.9)$$

and the  $m$ th logarithmic Richardson-Thomas transform as

TABLE VI. Donaldson-Thomas invariants.

| d/n | -3 | -2   | -1        | 0             | 1                 | 2                   |
|-----|----|------|-----------|---------------|-------------------|---------------------|
| 0   | 0  | 0    | 0         | 0             | 2875              | 569 250             |
| 1   | 0  | 0    | 0         | 0             | 609 250           | 124 762 875         |
| 2   | 0  | 0    | 0         | 609 250       | 439 056 375       | 76 438 831 000      |
| 3   | 0  | 8625 | 2 294 250 | 4 004 590 375 | 1 010 473 893 000 | 123 236 265 797 125 |

$$k_l^{(m)} = \frac{k_{l+1}^{(m-1)} \log(l+1) - k_l^{(m-1)} \log(l)}{\log(l+1) - \log(l)}. \quad (4.10)$$

With our knowledge of the topological string up to  $g = 31$  for the quintic we can evaluate the Donaldson-Thomas invariants up to degree 15. In the two graphs in Fig. 5, we plot the data for the  $k_l^{(0)}$  and its first two logarithmic Richardson-Thomas transforms. The graphs clearly indicate that the convergence is improved by the transform. So even if there are subleading terms of other forms, we

certainly managed to suppress the leading correction and speed up the convergence. The data further show that there is a universal behavior independent of  $d$  and that the value of  $k$  is within the 2% range close to 2. The higher logarithmic Richardson-Thomas transforms are consistent with this value but do not determine it better as we also have to take into account values with smaller  $l$  hence smaller  $\lambda$ . We next test the universality of these results for other charges  $(d, n)$  in Fig. 6. If  $n \neq 0$  we need the interpolation for the  $n'$  values. This introduces some random subleading errors,

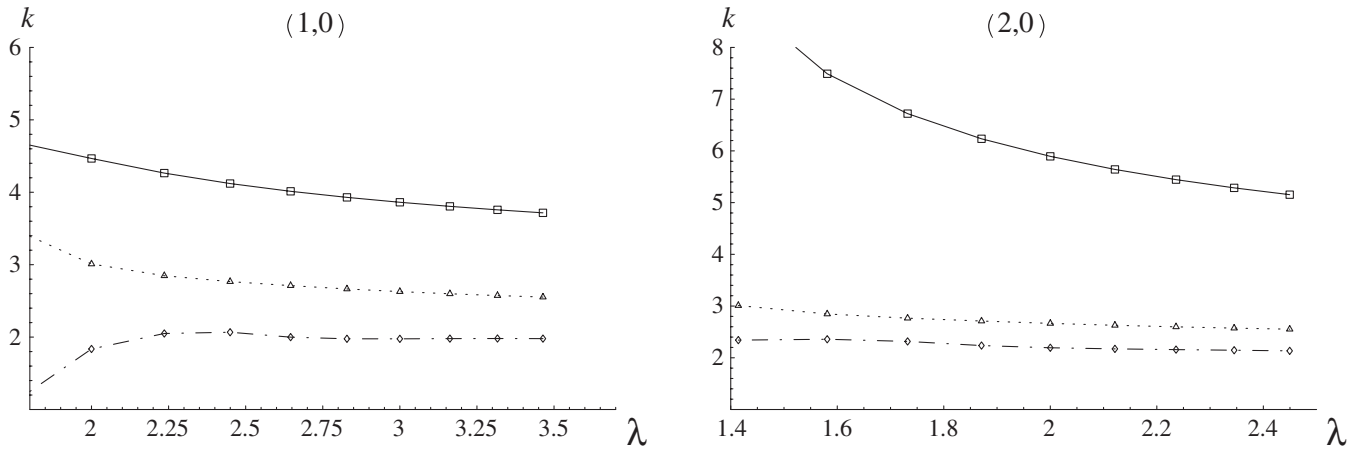


FIG. 5. Scaling data  $k^{(0)}$  ( $\square$ ) and the transforms  $k^{(1)}$  ( $\triangle$ ),  $k^{(2)}$  ( $\diamond$ ) for the Donaldson-Thomas invariants on the quintic in  $\mathbb{P}^4$  starting for  $(d, 0)$  states.

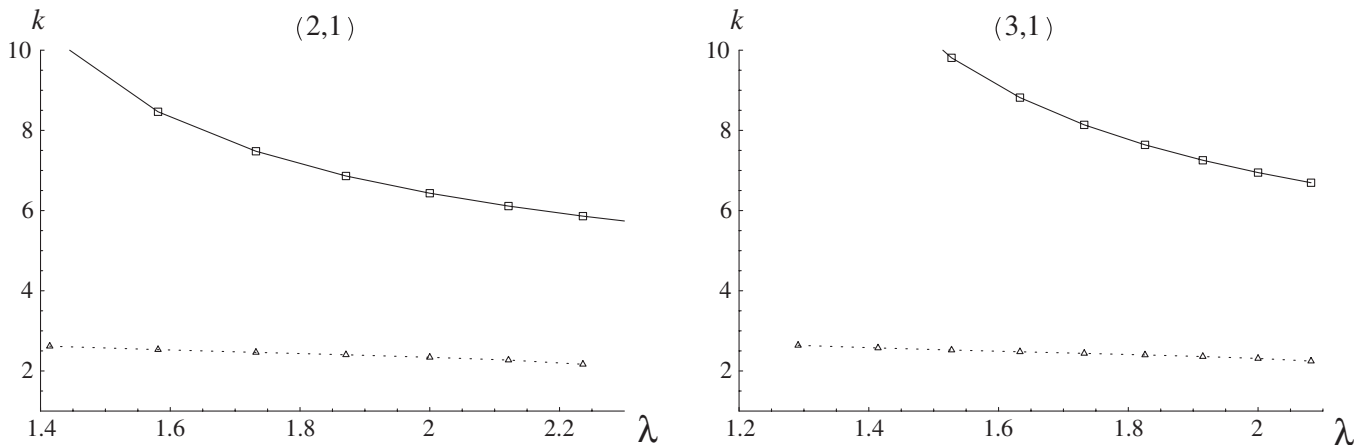


FIG. 6. Scaling data  $k^{(0)}$  ( $\square$ ) and the first transform  $k^{(1)}$  ( $\triangle$ ) for the Donaldson-Thomas invariants on the quintic in  $\mathbb{P}^4$  for the  $(2, 1)$  and  $(3, 1)$  states.

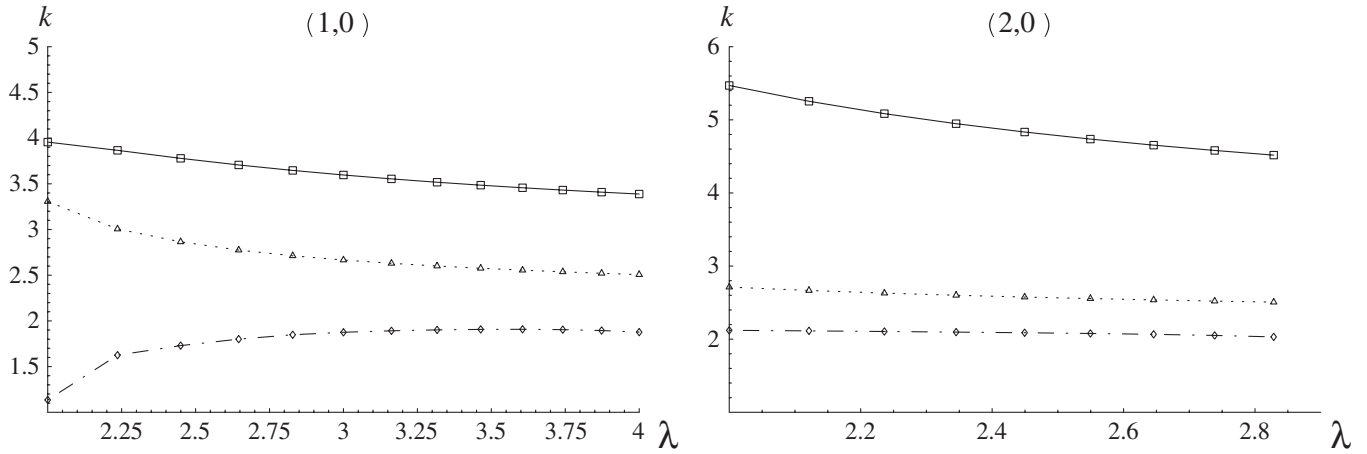


FIG. 7. Scaling data  $k^{(0)}$  ( $\square$ ) and the transforms  $k^{(1)}$  ( $\triangle$ ),  $k^{(2)}$  ( $\diamond$ ) for the Donaldson-Thomas invariants on the bicubic complete intersection in  $\mathbb{P}^5$  starting for  $(d, 0)$  states.

which are of the order of the improvement by the second logarithmic Richardson-Thomas transform. However, as in the figure for  $(2, 0)$  we see that higher  $d$  seems to lower the coefficient of the sub-subleading correction and makes already the second Richardson transform to converge reasonably well—well enough at least to conclude that the  $k$  is considerably lower than three and very well compatible with the value  $k = 2 \pm 0.03$  found for the previous charges. We solved the bicubic in  $\mathbb{P}^5$  up to genus 29, which yields complete information about the Donaldson-Thomas invariants up to degree 18. A similar analysis as above confirms the analysis for the quintic. The corresponding plots are in Figs. 7 and 8. Again a detailed summary of the data for more models can be found in [30]. We note a slight noise in the transform  $k^{(1)}$  in Fig. 8, which is presumably due to the interpolation in the  $n$  value of  $D_{d,n}$  described above. The results for the other models are similar, but somewhat less precise due to smaller values of  $d$  that are currently available.

To summarize: our analysis indicates that the value of  $k$  is indeed universal and close to  $k = 2$ . This strongly suggests that the “mysterious cancellations” [12] that eventually make it possible to extend the OSV conjecture to small coupling, actually take place.

## V. K3 FIBRATIONS

### A. Topological strings on K3 fibrations

We will now consider Calabi-Yau manifolds  $X$  that have the structure of a K3 fibration, i.e. there is a fibration of the form

$$\pi: X \rightarrow \mathbb{P}^1, \tag{5.1}$$

where the fibers are K3 surfaces. When the fibration is regular the homology of  $X$  can be written as

$$H_2(X, \mathbb{Z}) = \langle [\mathbb{P}^1] \rangle \oplus \text{Pic}(\text{K3}), \tag{5.2}$$

where  $\text{Pic}(\text{K3})$  is the Picard lattice of the K3 fiber. The rank

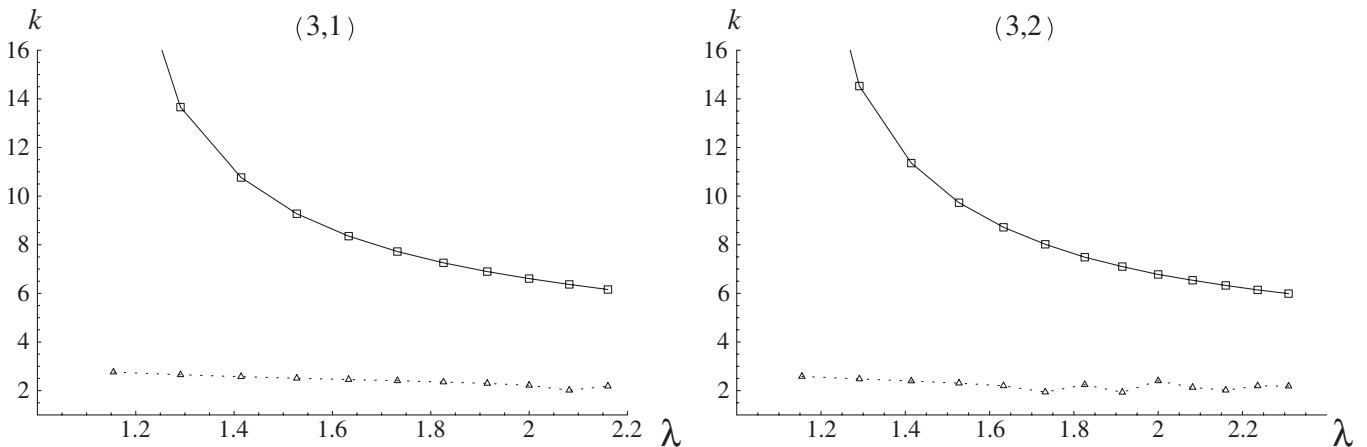


FIG. 8. Scaling data  $k^{(0)}$  ( $\square$ ) and the first transform  $k^{(1)}$  ( $\triangle$ ) for the Donaldson-Thomas invariants on the bicubic complete intersection in  $\mathbb{P}^5$  for the  $(3, 1)$  and  $(3, 2)$  states.

of this lattice will be denoted by  $\rho$ , and  $\Sigma^a$ ,  $a = 1, \dots, \rho$  will denote a basis for this lattice. Let  $\omega$  be the complexified Kähler form on  $X$ . The complexified Kähler parameters of  $X$  are given by

$$S = \int_{\mathbb{P}^1} \omega, \quad t^a = \int_{\Sigma^a} \omega, \quad a = 1, \dots, \rho. \quad (5.3)$$

We will denote by  $\eta_S, \eta_a$  the two-forms which are dual to  $\mathbb{P}^1, \Sigma^a$ .

It turns out that type IIA string theory compactified on these manifolds is very often dual to heterotic string theory compactified on  $K3 \times \mathbb{T}^2$  [34,35]. Under this duality,  $S$  becomes the axidilaton of the heterotic string. It follows that in the regime  $S \rightarrow \infty$  one can map computations in the type IIA theory to perturbative computations in the heterotic string. In particular, the  $F_g$  couplings of topological string theory (which are graviphoton couplings in type IIA theory) can be computed exactly at one loop in the heterotic string, provided the Kähler parameters are restricted to the K3 fiber [14,34–36]. We will now review here some of these results.

The topological string amplitudes  $F_g(S, t)$  on these fibrations have the following structure:

$$\begin{aligned} F_0(S, t) &= \frac{1}{6} C_{abc} t^a t^b t^c + \frac{1}{2} C_{ab} S t^a t^b + \frac{\zeta(3)}{2} \chi(X) \\ &\quad + \mathcal{F}_0(t) + \mathcal{O}(e^{-S}), \\ F_1(S, t) &= \frac{1}{24} (c_S S + c_a t^a) + \mathcal{F}_1(t) + \mathcal{O}(e^{-S}), \\ F_g(S, t) &= d_g \chi(X) + \mathcal{F}_g(t) + \mathcal{O}(e^{-S}), \quad g \geq 2. \end{aligned} \quad (5.4)$$

In these formulae,  $C_{abc}$  and  $C_{ab}$  are triple intersection numbers in the fiber and in the mixed fiber/base direction, respectively. Notice that

$$C_{abc} = \int_X \eta_a \wedge \eta_b \wedge \eta_c, \quad C_{ab} = \int_X \eta_S \wedge \eta_a \wedge \eta_b. \quad (5.5)$$

We also have

$$c_a = \int_X c_2(X) \wedge \eta_a, \quad a = 1, \dots, \rho, \quad c_S = \int_X c_2(X) \wedge \eta_S. \quad (5.6)$$

For K3 fibrations with trivial fundamental group one has  $c_S = 24$  [37], but for the Enriques Calabi-Yau manifold (which we will also analyze),  $c_S = 12$ . The coefficient  $d_g$  is the contribution of constant maps written down in (2.11). In (5.4),  $\mathcal{F}_g(t)$  denotes the contribution of world-sheet instantons in the K3 fiber. It follows from [14,16,18,36,38] that the  $\mathcal{F}_g(t)$  can be completely determined in terms of a single modular form that we will denote  $f_X(q)$ . In order to write down an explicit formula for  $\mathcal{F}_g(t)$ , we have to introduce the quasimodular forms  $\mathcal{P}_g(q)$  which are defined by

$$\left( \frac{2\pi\eta^3\lambda}{\vartheta_1(\lambda|\tau)} \right)^2 = \sum_{g=0}^{\infty} (2\pi\lambda)^{2g} \mathcal{P}_g(q). \quad (5.7)$$

The quantities  $\mathcal{P}_g(q)$  can be explicitly written in terms of generalized Eisenstein series [18], and one has, for example,

$$\mathcal{P}_1(q) = \frac{1}{12} E_2(q), \quad \mathcal{P}_2(q) = \frac{1}{1440} (5E_2^2 + E_4). \quad (5.8)$$

We now introduce the coefficients  $c_g(n)$  through

$$\mathcal{P}_g(q) f_X(q) = \sum_n c_g^X(n) q^n. \quad (5.9)$$

One then has the following expression for the heterotic  $\mathcal{F}_g(t)$ :

$$\mathcal{F}_g(t) = \sum_{Q \in \text{Pic}(K3)} c_g^X(Q^2/2) \text{Li}_{3-2g}(e^{-Q \cdot t}), \quad (5.10)$$

where  $\text{Li}_n$  is the polylogarithm of index  $n$

$$\text{Li}_n(x) = \sum_{k=1}^{\infty} \frac{x^k}{k^n}. \quad (5.11)$$

In (5.10) we have also denoted

$$Q \cdot t = n_a t^a, \quad Q^2 = C^{ab} n_a n_b, \quad (5.12)$$

where  $C^{ab} = C_{ab}^{-1}$  is the intersection form of the Picard lattice  $\text{Pic}(K3)$ .

We will be particularly interested in three special K3 fibrations: the STU model, the ST model, and the Enriques Calabi-Yau model. Let us give some extra details for these cases:

- (i) The STU model has  $\rho = 2$  and it can be realized by a complete intersection in a weighted projective space which is frequently denoted by  $X_{24}(1, 1, 2, 8, 12)$ . It has Euler characteristic  $\chi = -480$ . The classical prepotential can be obtained from the nonvanishing intersection numbers,

$$C_{111} = 8, \quad C_{112} = 2, \quad C_{11} = 2, \quad C_{12} = 1, \quad (5.13)$$

while the classical part of  $F_1(S, t)$  is encoded by

$$c_1 = 92, \quad c_2 = c_S = 24. \quad (5.14)$$

The modular form encoding the information about topological string amplitudes in the fiber is given by [18]

$$f_{\text{STU}}(q) = -\frac{2E_4 E_6}{\eta^{24}}(q). \quad (5.15)$$

It is sometimes useful to parametrize the Kähler cone in terms of the variables

$$T = t_1 + t_2, \quad U = t_1. \quad (5.16)$$

In this basis one has  $Q^2/2 = mn$ .

- (ii) The ST model has  $\rho = 1$  and is realized in type IIA by the CY model  $X_{12}(1, 1, 2, 2, 6)$ . It has  $\chi = -252$  and the classical intersection numbers

$$C_{111} = 4, \quad C_{11} = 2, \quad (5.17)$$

as well as

$$c_1 = 52, \quad c_S = 24. \quad (5.18)$$

The Kähler parameter along the fiber is usually denoted as

$$T = t_1. \quad (5.19)$$

The relevant modular form is [16,38]

$$f_{\text{ST}}(q) = -\frac{2\theta E_4 F_6}{\eta^{24}}(q), \quad (5.20)$$

where

$$\begin{aligned} \theta(q) &= \sum_{n \in \mathbb{Z}} q^{n^2/4} = \vartheta_3(\tau/2), & F_2 &= \frac{1}{16} \vartheta_2^4(\tau/2), \\ F_6 &= E_6 - 2F_2(\theta^4 - 2F_2)(\theta^4 - 16F_2). \end{aligned} \quad (5.21)$$

Notice that  $Q^2/2 = n^2/4$ .

- (iii) The Enriques Calabi-Yau model is given by the free quotient  $(\text{K3} \times \mathbb{T}^2)/\mathbb{Z}_2$ , and was introduced in the context of type II/heterotic duality in [39]. It is an elliptic fibration with  $\rho = 10$ . It has  $C_{abc} = 0$ , while  $C_{ab}$  is given by the intersection numbers of the Enriques surface  $E$ . The Picard lattice is

$$\text{Pic}(\text{K3}) = \Gamma^{1,1} \oplus E_8(-1), \quad (5.22)$$

and

$$c_a = 0, \quad c_S = 12. \quad (5.23)$$

The topological string amplitudes in the fiber were obtained in [17] (see also [15]). They are also controlled by a single modular form

$$f_E(q) = -\frac{2}{\eta^{12}(q^2)}, \quad (5.24)$$

but their form is slightly different from (5.10)

$$\begin{aligned} F_g(t) &= \sum_{Q \in \text{Pic}(\text{K3})} c_g^E(Q^2) \{2^{3-2g} \text{Li}_{3-2g}(e^{-Q \cdot t}) \\ &\quad - \text{Li}_{3-2g}(e^{-2Q \cdot t})\}, \end{aligned} \quad (5.25)$$

where  $c_g^E(n)$  are defined again by (5.9).

## B. Microscopic degeneracies and their asymptotic expansion

We have seen that, at least in the case of topological strings on K3 fibrations, and for classes  $Q$  restricted to the K3 fiber, one can obtain closed formula for the topological string amplitudes at all genera. It should be therefore possible to extract a closed formula for the generating

functional of Gopakumar-Vafa invariants. In fact, by using the product formula

$$\begin{aligned} \vartheta_1(\nu|\tau) &= -2q^{1/8} \sin(\pi\nu) \prod_{n=1}^{\infty} (1 - q^n) \\ &\quad \times (1 - 2\cos(2\pi\nu)q^n + q^{2n}) \end{aligned} \quad (5.26)$$

one finds from the expression (5.10) and the structure (2.20)

$$\sum_{Q \in \text{Pic}(\text{K3})} \sum_{r=0}^{\infty} n_Q^r z^{2r} p^{Q^2/2} = f_X(p) \xi^2(z), \quad (5.27)$$

where  $\xi(z)$  is the function that appears in helicity supertraces,

$$\begin{aligned} \xi(z) &= \prod_{n=1}^{\infty} \frac{(1 - p^n)^2}{(1 - p^n)^2 + z^2 p^n} \\ &= \prod_{n=1}^{\infty} \frac{(1 - p^n)^2}{(1 - p^n y)(1 - p^n y^{-1})}, \end{aligned} \quad (5.28)$$

where we have set  $z = -i(y^{1/2} - y^{-(1/2)})$ .

We can now obtain a closed formula for the microscopic degeneracies. In order to have a description which incorporates as well the elliptic genus, we will count the microstates as in (2.18) but with  $r \rightarrow r - 1$ . With this definition, the left-hand side of (5.27), expanded in  $q, y$ , is precisely the generating function of microscopic degeneracies  $\Omega(Q, m)$ , summed over all  $m, Q$ . We then arrive at the expression

$$\sum_{Q \in \text{Pic}(\text{K3})} \sum_{m=-\infty}^{\infty} \Omega(Q, m) y^m p^{Q^2/2} = f_X(p) \xi^2(\nu, \sigma), \quad (5.29)$$

where we have written

$$y = e^{2\pi i \nu}, \quad p = e^{2\pi i \sigma}. \quad (5.30)$$

Notice that if we consider  $X = \text{K3} \times \mathbb{T}^2$  and restrict to classes  $Q$  in the fiber, the counting of microstates given by the elliptic genus is

$$\begin{aligned} \chi(S_p \text{K3}; q, y)_{q^0} &= \prod_{N=1}^{\infty} \frac{1}{(1 - p^N)^{20} (1 - p^N y)^2 (1 - p^N y^{-1})^2} \\ &= \frac{P}{\eta^{24}(p)} \xi^2(y). \end{aligned} \quad (5.31)$$

This has the same form as (5.29) with

$$f_{\text{K3} \times \mathbb{T}^2}(p) = \frac{1}{\eta^{24}(p)}, \quad (5.32)$$

therefore we can consider the ‘‘small’’ D1-D5 system as a particular case of our analysis.

The expression (5.29) tells us that the microscopic degeneracies we are looking for are simply the Fourier coefficients of the object in the right-hand side. We can then

invert it to write

$$\Omega(N, m) = \int_{-(1/2)+i0^+}^{(1/2)+i0^+} d\sigma \int_0^1 d\nu e^{-2\pi i(N\sigma+m\nu)} \Phi(\nu, \sigma),$$

$$N = Q^2/2, \quad (5.33)$$

where we defined

$$\Phi(\nu, \sigma) = f_X(p) \xi^2(\nu, \sigma), \quad (5.34)$$

and we have assumed that  $N$  is a non-negative integer (this can be guaranteed by rescaling  $p \rightarrow p^k$  for some appropriate  $k$ ). The contour in (5.33) has been chosen to avoid the poles in the integrand.

We will now evaluate the asymptotic expansion of  $\Omega(N) \equiv \Omega(N, 0)$  in inverse powers of  $N$ . Nonzero values of the spin  $m = 0$  can be analyzed in a similar way. The expression we will find is exact up to corrections which are exponentially suppressed in the large charge limit  $N \rightarrow \infty$ . Notice that in our situation we cannot appeal to the Rademacher expansion which was used in [19,20], since (5.34) is not a Jacobi form (it can be regarded as a Jacobi form with *negative* index). It is likely that an analog of the Rademacher expansion exists, but we will perform a direct evaluation of the integral (5.33) in the spirit of the counting of states with spin in Appendix C of [19] and in [40].

First of all, we reexpress the integrand (5.34) in terms of  $\vartheta_1(\nu|\sigma)$  as

$$\Phi(\nu, \sigma) = 4\sin^2(\pi\nu) \eta^6(p) \frac{f_X(p)}{\vartheta_1^2(\nu|\sigma)}. \quad (5.35)$$

Using the modular behavior of  $\vartheta_1(\nu|\sigma)$  under the  $S$  transformation  $\sigma \rightarrow \tilde{\sigma} = -1/\sigma$  we get

$$\vartheta_1(\nu, \sigma) = -\frac{2i}{\sqrt{-i\sigma}} e^{(\pi/i\sigma)(\nu^2+(1/4))} \sin\left(\frac{\pi\nu}{\sigma}\right)$$

$$\times \left\{ 1 + O(e^{-(2\pi i/\sigma)}) \right\}. \quad (5.36)$$

It is easy to see that the saddle point evaluation of (5.33) is governed by

$$\sigma_* = \frac{i}{\sqrt{N}} + \mathcal{O}\left(\frac{1}{N}\right). \quad (5.37)$$

Therefore, the corrections to (5.36) will be exponentially suppressed. Using the modularity of  $\eta(p)$  and taking the part of the sin in the denominator which is not exponentially suppressed, we obtain

$$\Phi(\nu, \sigma) \sim -4\sigma^{-2} e^{2(i\pi/\sigma)(\nu^2-\nu)} \sin^2(\pi\nu) f_X(p). \quad (5.38)$$

Therefore, in order to compute the asymptotics of (5.33) we just need

$$\Omega(N) \sim -4 \int_{-(1/2)+i0^+}^{(1/2)+i0^+} d\sigma e^{-2\pi i N \sigma} \frac{f_X(p)}{\sigma^2}$$

$$\times \int_0^1 d\nu e^{2(i\pi/\sigma)(\nu^2-\nu)} \sin^2(\pi\nu). \quad (5.39)$$

The integral over  $\nu$  is easily worked out in terms of the error function  $\text{Erf}(x)$ , as follows:

$$\int_0^1 d\nu e^{2(i\pi/\sigma)(\nu^2-\nu)} \sin^2(\pi\nu) = \sqrt{\frac{i\sigma}{8}} e^{(\pi/2i\sigma)} \text{Erf}\left(\sqrt{\frac{\pi}{2i\sigma}}\right)$$

$$+ \sqrt{\frac{i\sigma}{32}} e^{(\pi/2i)(\sigma+(1/\sigma))}$$

$$\times \left\{ \text{Erf}\left(\sqrt{\frac{\pi}{2i\sigma}}(\sigma+1)\right) - \text{Erf}\left(\sqrt{\frac{\pi}{2i\sigma}}(\sigma-1)\right) \right\}. \quad (5.40)$$

Because of (5.37) we can use the asymptotic expansion of the Erf function,

$$\text{Erf}(x) \sim 1 - \frac{e^{-x^2}}{\sqrt{\pi}} \sum_{r=0}^{\infty} (-1)^r \frac{(2r-1)!!}{2^r} x^{-(2r+1)},$$

$$|x| \rightarrow \infty, |\arg(-x)| < \pi. \quad (5.41)$$

Ignoring terms which are exponentially suppressed at large  $N$ , we find

$$\int_0^1 d\nu e^{2(i\pi/\sigma)(\nu^2-\nu)} \sin^2(\pi\nu) \sim -\frac{1}{4} \sum_{r=0}^{\infty} \frac{i^{1+3r}}{\pi^{1+r}} (2r-1)!!$$

$$\times G_r(\sigma), \quad (5.42)$$

with

$$G_r(\sigma) = \sigma^{r+1} \left( 2 + \frac{1}{(\sigma-1)^{1+2r}} - \frac{1}{(\sigma+1)^{1+2r}} \right). \quad (5.43)$$

Again, due to (5.37), we can expand it around  $\sigma = 0$ ,

$$G_r(\sigma) = -2 \sum_{s=0}^{\infty} \binom{2(1+s+r)}{2r} \sigma^{3+2s+r}. \quad (5.44)$$

Putting all together, we obtain

$$\Omega(N) \sim 2 \sum_{r=0}^{\infty} \frac{(2r-1)!!}{(i\pi)^{r+1}} \sum_{s=0}^{\infty} \binom{2(1+s+r)}{2r}$$

$$\times \int_{-(1/2)+i0^+}^{(1/2)+i0^+} d\sigma e^{-2\pi i N \sigma} f_X(p) \sigma^{1+2s+r}. \quad (5.45)$$

We now work out the integral

$$A_{s,r}(N) \equiv \int_{-(1/2)+i0^+}^{(1/2)+i0^+} d\sigma e^{-2\pi i N \sigma} f_X(p) \sigma^{1+2s+r}. \quad (5.46)$$

We assume that  $f_X(p)$  has modular weight  $w$ , so that  $f_X(p) = \sigma^{-w} f_X(\tilde{p})$ , where  $\tilde{p} = e^{-(2\pi i/\sigma)}$ . For the modular forms that we consider here,  $f_X(\tilde{p}) = c \tilde{p}^{-\alpha} + \dots$ , and the integral above gives a modified Bessel function

$$A_{s,r}(N) \sim c i^{1+2s+r-w} \hat{I}_{2s+r+2-w}(4\pi\sqrt{\alpha N}). \quad (5.47)$$

We end up then with the following result for the exact

asymptotics of the microscopic black hole degeneracy:

$$\Omega(N) \sim 2ci^w \sum_{r=0}^{\infty} \frac{(2r-1)!!}{\pi^{r+1}} \sum_{s=0}^{\infty} (-1)^s \binom{2(1+s+r)}{2r} \times \hat{I}_{2s+r+2-w}(4\pi\sqrt{\alpha N}). \quad (5.48)$$

Using now the formula for the asymptotic expansion of  $\hat{I}$  functions (see, for example, Appendix A of [19]), we find for the entropy  $S(N) = \log\Omega(N)$  the following expansion:

$$S \sim 4\pi\sqrt{\alpha N} - \frac{5-2w}{4} \log(N) + \log\left(\frac{\sqrt{2i}^w \alpha^{(2w-5/4)c}}{\pi}\right) + \frac{177+16w-4w^2}{32\pi\sqrt{\alpha}} \frac{1}{\sqrt{N}} + \mathcal{O}(N^{-1}). \quad (5.49)$$

The expansion in powers of  $1/N^{1/2}$  in (5.48), which is obtained by using the asymptotics of modified Bessel functions, is the expansion of the original integral around the saddle point (5.37). This can be verified by an explicit computation of the first few orders of the saddle point expansion.

Let us now evaluate (5.49) in some examples. For K3  $\times$   $\mathbb{T}^2$  we have  $(w, \alpha, c) = (-12, 1, 1)$ , and the entropy reads

$$S \sim 4\pi\sqrt{N} - \frac{29}{4} \log(N) + \log\left(\frac{\sqrt{2}}{\pi}\right) - \frac{591}{32\pi} \frac{1}{\sqrt{N}} + \mathcal{O}(N^{-1}). \quad (5.50)$$

For the STU model, with the values  $(w, \alpha, c) = (-2, 1, -2)$ , we find

$$S \sim 4\pi\sqrt{N} - \frac{9}{4} \log(N) + \log\left(\frac{\sqrt{8}}{\pi}\right) + \frac{129}{32\pi} \frac{1}{\sqrt{N}} + \mathcal{O}(N^{-1}). \quad (5.51)$$

The ST model is slightly different, since in  $f_{ST}(p)$  both integer and rational powers of  $p$  appear. As mentioned above, we should redefine  $p \rightarrow p^4$  and write down the generating functional for the degeneracies as

$$\sum_{Q \in \text{Pic}(K3)} \sum_{m=-\infty}^{\infty} \Omega(Q, m) y^m p^{2Q^2} = f_{ST}(p^4) \xi^2(\nu, 4\sigma), \quad (5.52)$$

where we recall that  $M \equiv 2Q^2 = n^2$  is an integer. The asymptotics is given by the integral

$$\Omega_{ST}(M) \sim - \int_{-(1/2)+i0^+}^{(1/2)+i0^+} d\sigma e^{-2\pi i M \sigma} \frac{f_{ST}(p^4)}{4\sigma^2} \times \int_0^1 d\nu \sin^2(\pi\nu) e^{(i\pi/2\sigma)(\nu^2-\nu)}. \quad (5.53)$$

The integral over  $\nu$  is given by (5.40) upon replacing  $\sigma \rightarrow 4\sigma$ . Since

$$f_{ST}(p^4) = -2 \frac{E_4(p^4) F_6(p^4)}{\eta^{24}(p^4)} \vartheta_3(2\sigma) \sim -16\sqrt{2i} \sigma^{3/2} e^{(i\pi/2\sigma)}, \quad (5.54)$$

one finds in the end

$$\Omega_{ST}(M) \sim \sqrt{2} \sum_{r=0}^{\infty} \frac{(2r-1)!!}{\pi^{r+1}} \sum_{s=0}^{\infty} (-1)^s \binom{2(1+s+r)}{2r} \times \hat{I}_{(7/2)+2s+r}(2\pi\sqrt{M}), \quad (5.55)$$

and from here one can read the entropy

$$S(Q) \sim 4\pi\sqrt{\frac{1}{2}Q^2} - 2 \log(Q^2) + \dots \quad (5.56)$$

Finally we turn to the case of Enriques CY manifold. It follows from (5.25) that one has to distinguish two types of homology classes: the classes  $Q$  whose entries contain at least an odd integer (which were called odd classes in [17]), and the classes  $Q$  for which all entries are even (called even classes). A simple calculation shows that the generating function of Gopakumar-Vafa invariants for the odd classes is given by

$$\sum_{r=0}^{\infty} \sum_{Q \text{ odd}} n_Q^r p^{Q^2} z^{r-1} = \frac{f_E(q)}{4\sin^2(\frac{\pi\nu}{2})} (\xi^2(\nu/2, p) - \xi^2(\nu/2, -p)), \quad (5.57)$$

while for the even classes is given by

$$\sum_{r=0}^{\infty} \sum_{Q \text{ even}} n_Q^r p^{Q^2} z^{r-1} = \frac{f_E(q)}{4\sin^2(\frac{\pi\nu}{2})} (\xi^2(\nu/2, p) - \xi^2(\nu/2, -p)) - f_E(q^4) \times (\xi^2(\nu, p^4) - \xi^2(\nu, -p^4)). \quad (5.58)$$

Notice that for even classes  $Q^2 \equiv 0 \pmod{4}$ , while for odd classes one only has  $Q^2 \equiv 0 \pmod{2}$ . In contrast to the previous K3 fibrations, in the above generating function we have  $p^{Q^2}$ , instead of  $p^{Q^2/2}$ , and this will lead to a different leading term as compared, for example, to the STU model.

The computation of the asymptotics of the microstates is similar to the one that we just performed. Let us begin with odd classes. Using the identity

$$\xi^2(\nu, -p) = 4\sin^2(\pi\nu) \frac{\eta^6(2\sigma) \vartheta_3^2(2\sigma)}{\vartheta_1^2(\nu|2\sigma) \vartheta_3^2(\nu|2\sigma)}, \quad (5.59)$$

and proceeding as in the previous case, we find

$$\Omega_{\text{odd}}(N) = \Omega_1(N) + \Omega_2(N), \quad N = Q^2/2, \quad (5.60)$$

where



$$\begin{aligned}\Omega_1(N) &\sim 16 \int_{-(1/2)+i0^+}^{(1/2)+i0^+} d\sigma e^{-4\pi i N \sigma} \sigma^2 \eta^6(2\sigma) \vartheta_3^2(2\sigma) f_E(p) \\ &\quad \times \int_0^1 d\nu \sin^2(\pi\nu) e^{(i\pi/2\sigma)(\nu^2 - \nu + (1/2))}, \\ \Omega_2(N) &\sim -4i \int_{-(1/2)+i0^+}^{(1/2)+i0^+} d\sigma e^{-4\pi i N \sigma} \sigma \eta^6(\sigma) f_E(p) \\ &\quad \times \int_0^1 d\nu \sin^2(\pi\nu) e^{(i\pi/2\sigma)(\nu-1)^2}.\end{aligned}\quad (5.61)$$

As before, we evaluate the integrals over  $\nu$  in terms of the Erf function and its asymptotic expansion. We then use the modularity properties of the different functions involved here to obtain

$$\begin{aligned}\Omega_{\text{odd}}(N) &\sim \frac{1}{16} \sum_{r=0}^{\infty} \frac{(2r-1)!!}{\pi^{r+1}} \sum_{s=0}^{\infty} (-1)^s \binom{2(1+s+r)}{2r} \\ &\quad \times (1 - 4^{-(1+r+s)}) \hat{I}_{8+2s+r}(\pi\sqrt{8N}).\end{aligned}\quad (5.62)$$

Let us now consider the even classes, (5.58). Comparing (5.58) with (5.57), we see that

$$\Omega_{\text{even}}(N) = \Omega_{\text{odd}}(N) - \tilde{\Omega}(N),\quad (5.63)$$

where

$$\begin{aligned}\tilde{\Omega}(N) &= \int_{-(1/2)+i0^+}^{(1/2)+i0^+} d\sigma \int_0^1 d\nu e^{-4i\pi N \sigma} 4\sin^2(\pi\nu) f_E(p^4) \\ &\quad \times (\xi^2(\nu, p^4) - \xi^2(\nu, -p^4)).\end{aligned}\quad (5.64)$$

A computation similar to the one we performed shows that  $\tilde{\Omega}(N)$  is exponentially suppressed with respect to  $\Omega_{\text{odd}}(N)$ , since it leads to terms that go like  $\exp(\pi\sqrt{2N})$  and  $\exp(\pi\sqrt{6N})$ . Therefore, as an asymptotic expansion in  $1/\sqrt{N}$ ,  $\Omega_{\text{even}}(N) \sim \Omega_{\text{odd}}(N)$ , and the asymptotics does not distinguish between the even and the odd classes. We finally obtain, for the small Enriques black hole,

$$S_E(Q) \sim 2\pi\sqrt{Q^2} - \frac{17}{2}\log\sqrt{Q^2} + \dots\quad (5.65)$$

The main conclusion of our analysis is that, in all cases, the leading term of the microscopic entropy for these black holes is given by

$$S(Q) \sim 2\pi\sqrt{\frac{c_S}{12}Q^2},\quad (5.66)$$

since  $c_S = 24$  for  $\text{K3} \times \mathbb{T}^2$ , the STU and the ST models, but  $c_S = 12$  for the Enriques CY model. Of course, our analysis has also given precise formulae for the subleading terms.

The leading behavior (5.66) can be also verified by a numerical analysis similar to the one performed in Secs. III and IV. For example, for the STU model we have computed the quantity  $f(N) = S(N)/\sqrt{N}$  for  $1 \leq N < 50$ , where  $S(N) = \log\Omega(N)$ . In order to subtract the logarithmic term in the asymptotic expansion (5.51) we consider the transform

$$A(N) = \frac{(N+1)S(N+2) - (2N+1)S(N+1) + NS(N)}{(N+1)\sqrt{N+2} - (2N+1)\sqrt{N+1} + N\sqrt{N}}.\quad (5.67)$$

In Fig. 9 we plot  $f(N)$  (bottom) and  $A(N)$  (top). The horizontal line is the expected asymptotic value  $4\pi$  for both quantities as  $N \rightarrow \infty$ . As before, the transform  $A(N)$  improves rapidly the convergence.

### C. Macroscopic entropy for small black holes

The 5d black holes obtained by wrapping the M2 branes along cycles in the K3 fiber have actually vanishing classical entropy and are therefore *small* black holes. Indeed, as we have seen, the leading asymptotic degeneracy scales like  $Q$ , and not like  $Q^{3/2}$ . This is also what is found for small 4d black holes [19].

Let us briefly show that the classical area of these black holes is zero for any set of intersection numbers  $C_{abc}$ ,  $C_{ab}$ . In order to do this, we can use the 5d attractor mechanism described in Sec. II. Equivalently, by using the 4d/5d connection of [21], we can map the 5d black hole to a 4d black hole with D6 charge  $p^0 = 1$  and D2 charges  $Q_A$ . At the level of the leading macroscopic entropy, the 4d computation gives the same result as the 5d computation [21]. In the 4d language, we start with the tree-level SUGRA prepotential

$$F = -\frac{1}{2}C_{ab}\frac{X^S X^a X^b}{X^0} - \frac{1}{6}C_{abc}\frac{X^a X^b X^c}{X^0}.\quad (5.68)$$

We will do the computation for a generic D6-D2 charge, i.e. we will start with generic charges  $p^0$ ,  $Q_a$ ,  $Q_S$ , and then take the charge  $Q_S \rightarrow 0$  at the end of the computation (as well as setting  $p^0 = 1$ ). This will guarantee that we obtain generic solutions to the attractor mechanism.

Let us first assume that  $C_{abc} = 0$ , as it happens in  $\text{K3} \times \mathbb{T}^2$  and the Enriques Calabi-Yau manifold. In this case, the attractor equations are easily solved as

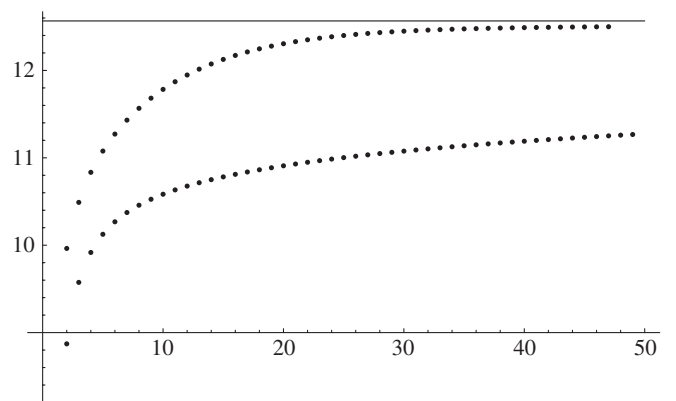


FIG. 9. Microscopic data for  $f(N) = S(N)/\sqrt{N}$  (bottom) and its transform  $A(N)$  (top), defined in (5.67), for the STU model, and for  $1 \leq N < 50$ . The horizontal line is the expected asymptotic value  $4\pi$ .

$$(X_*^0, X_*^S, X_*^a) = \left( p^0, i\sqrt{\frac{p^0 Q^2}{2Q_S}}, i\sqrt{\frac{2Q_S p^0}{Q^2}} Q^a \right), \quad (5.69)$$

where

$$Q^2 = C^{ab} Q_a Q_b, \quad Q^a = C^{ab} Q_b. \quad (5.70)$$

The entropy is given by

$$S = \pi\sqrt{2p^0 Q_S Q^2}, \quad (5.71)$$

and it vanishes in the limit  $Q_S \rightarrow 0$ . This is as expected.

If we now consider a general prepotential with non-vanishing  $C_{abc}$ , the attractor equations are now solved at

$$(X^0, X^S, X^a) = \left( p^0, i\sqrt{\frac{p^0}{2Q_S}} \xi^S, i\sqrt{2p^0 Q_S} \xi^a \right), \quad (5.72)$$

where the  $\xi^A$  are solutions to

$$\xi^a \xi_a = 1, \quad Q^a = \xi^S \xi^a + Q_S C^{ab} C_{bef} \xi^e \xi^f. \quad (5.73)$$

Notice that, in these variables, the model with  $C_{abc} = 0$  corresponds to the smooth values,

$$(\xi_*^S, \xi_*^a) = \left( \sqrt{Q^2}, \frac{Q^a}{\sqrt{Q^2}} \right). \quad (5.74)$$

We can already see that, in the limit  $Q_S \rightarrow 0$ , the perturbation by  $C_{abc}$  in (5.73) vanishes, therefore in the limit of zero charge in the base the presence of nontrivial intersection numbers in the fiber should be unimportant. More formally, it is easy to see that one can construct a consistent solution of (5.73) of the form

$$\xi^A = \xi_*^A + \sum_{n=1}^{\infty} c_n^A Q_S^n, \quad (5.75)$$

where the coefficients  $c_n^A$  depend on  $C_{abc}$  and can be calculated order by order. In terms of the  $\xi^A$  the macroscopic entropy is

$$S = \pi\sqrt{2p^0 Q_S (C_{ab} \xi^a \xi^b \xi^S + \frac{2}{3} Q_S C_{abc} \xi^a \xi^b \xi^c)}, \quad (5.76)$$

and, in the limit  $Q_S \rightarrow 0$ , it will vanish irrespectively of the value of  $C_{abc}$ . Therefore, 5d black holes whose membrane charge is restricted to the K3 fiber of a K3 fibration are always small. This can be checked as well by detailed computations in different models (like the STU and ST models considered above).

Since the leading contribution to the entropy vanishes we should now look at the subleading terms in the macroscopic entropy. As we explained in Sec. II, it was shown in [23,25,26] that these terms are obtained by performing the shift

$$Q_A \rightarrow \hat{Q}_A = Q_A + \zeta c_{2A}, \quad \zeta = \frac{1}{8}. \quad (5.77)$$

The leading term in the entropy for the small 5d black hole is given (for large charge  $Q$ ) by performing this shift in (5.71)

$$S = 2\pi\sqrt{\frac{\zeta c_S}{2}} Q^2. \quad (5.78)$$

This can be derived in detail by solving the attractor equations with shifted charges (5.77) as a power series in  $1/Q$ , and then taking the limit  $Q_S \rightarrow 0$ . Notice that the entropy (5.78) only depends on  $C_{ab}$  and  $c_S$ . Also, in this regime, the solutions of the attractor equations occur at values of the Kähler parameters which are of the order of the string size, and the SUGRA calculation might be problematic. Indeed, it is easy to see that (5.78) does *not* agree with the leading term of the asymptotics that we obtained in the previous subsection. By comparing (5.66) with (5.78) we find that the formula agree if we set instead  $\zeta = 1/6$ . This is the value of  $\zeta$  that is predicted by the 4d/5d connection of [21].

In [23,26] it was noticed that the subleading correction (5.77) obtained in a macroscopic 5d computation was not in accord with the subleading correction predicted by [21] and the 4d attractor mechanism. We now find that, for *big* 5d black holes, the subleading correction for the microscopic entropy is in rough agreement with (5.77), while for *small* 5d black holes the leading asymptotics is in accord with a 4d computation for a small D6/D2 system with  $p^0 = 1$ . As we already mentioned, in the case of small black holes, the SUGRA computations with which we are comparing our results should receive large corrections, but in other situations they still lead to results which are in agreement with the microscopic counting, as in [19,41]. In our case we obtain a result in disagreement with the 5d computation but in agreement with the 4d computation. It would be interesting to resolve this puzzle.

## VI. CONCLUSIONS

In this paper we have studied the microscopic counting of 5d black hole states by using topological string theory. In the case of big black holes, we have given convincing numerical evidence that the BPS invariants encoded in the topological string amplitudes account correctly for the macroscopic entropy of spinning black holes. Moreover, we have also shown that the data favor the ‘‘mysterious cancellation’’ of [12] that makes it possible to extend the validity of the OSV conjecture, and we were able to explore new aspects of black hole entropy which have not been studied before using supergravity. Clearly, it would be very desirable to improve our numerical results with more data. Using the interplay between modularity and anholomorphicity in topological string theory [7,15,29], analytic results on the asymptotics might not be out of reach.<sup>4</sup>

<sup>4</sup>Recently beautiful analytic proofs of the asymptotic of the Fourier coefficients of Mock-Theta functions have been obtained using a somewhat similar interplay [42].

We also gave exact formulae for microscopic degeneracies of a class of small 5d black holes, which are obtained by wrapping M2 branes in the fiber of a K3 fibration, and we computed the asymptotic expansion in inverse powers of the charge. As expected, the calculation shows that for small black holes the leading term in the entropy scales like  $S \rightarrow \lambda S$  when the charges are scaled with  $\lambda$ . We found, however, that the coefficient of the leading term does not agree with the shift of charges obtained in [23,25,26] in a 5d SUGRA computation. In principle there is no reason why these two computations should agree, since small  $\mathcal{N} = 1$  black holes are generically beyond the SUGRA approximation. On the other hand, the microscopic results are well reproduced by the 4d/5d connection of [21] and a 4d attractor computation. We should emphasize, however, that for big black holes the 5d shift (5.77) fits our data better than the 4d shift with  $\zeta = 1/6$ . It would be very interesting to understand this better.

**ACKNOWLEDGMENTS**

It is a pleasure to thank Davide Gaiotto, Thomas Grimm, Aki Hashimoto, Sheldon Katz, Wei Li, Boris Pioline, Nick Warner, and Xi Yin for helpful discussions, and Frederik Denef for very useful correspondence. We would like to thank as well Gregory Moore and Cumrun Vafa for their comments on the manuscript. Many thanks also to Max Kreuzer for generously granting us computer time. This work is partially supported by DOE Grant No. DE-F602-95ER40896. A.T. is supported by a Marie Curie fellowship.

**APPENDIX: GENERAL FEATURES OF THE INSTANTON EXPANSION**

The asymptotic behavior at the conifold, Castelnuovo’s theory, and the calculation via degenerate Jacobians, suggest some general features of the Gopakumar-Vafa expansion. Our data for the 13 one-parameter models suggest further universal features. The purpose of this appendix is

TABLE VII. Gopakumar-Vafa invariants  $n_d^g$  in the class  $d = 18$  for the complete intersection  $X_{3,3}(1^6)$ .

| Genus | Degree = 18   |
|-------|---|
| 0     | 144 519 433 563 613 558 831 955 702 896 560 953 425 168 536 |
| 1     | 491 072 999 366 775 380 563 679 351 560 645 501 635 639 768 |
| 2     | 826 174 252 151 264 912 119 312 534 610 591 771 196 950 790 |
| 3     | 866 926 806 132 431 852 753 964 702 674 971 915 498 281 822 |
| 4     | 615 435 297 199 681 525 899 637 421 881 792 737 142 210 818 |
| 5     | 306 990 865 721 034 647 278 623 907 242 165 669 760 227 036 |
| 6     | 109 595 627 988 957 833 331 561 270 319 881 002 336 580 306 |
| 7     | 28 194 037 369 451 582 477 359 532 618 813 777 554 049 181  |
| 8     | 5 218 039 400 008 253 051 676 616 144 507 889 426 439 522   |
| 9     | 688 420 182 008 315 508 949 294 448 691 625 391 986 722     |
| 10    | 63 643 238 054 805 218 781 380 099 115 461 663 133 366      |
| 11    | 4 014 173 958 414 661 941 560 901 089 814 730 394 394       |
| 12    | 166 042 973 567 223 836 846 220 100 958 626 775 040         |
| 13    | 4 251 016 225 583 560 366 557 404 369 102 516 880           |
| 14    | 61 866 623 134 961 248 577 174 813 332 459 314              |
| 15    | 451 921 104 578 426 954 609 500 841 974 284                 |
| 16    | 1 376 282 769 657 332 936 819 380 514 604                   |
| 17    | 1 186 440 856 873 180 536 456 549 027                       |
| 18    | 2 671 678 502 308 714 457 564 208                           |
| 19    | -59 940 727 111 744 696 730 418                             |
| 20    | 1 071 660 810 859 451 933 436                               |
| 21    | -13 279 442 359 884 883 893                                 |
| 22    | 101 088 966 935 254 518,                                    |
| 23    | -372 702 765 685 392  |
| 24    | 338 860 808 028   |
| 25    | 23 305 068  |
| 26    | -120 186  |
| 27    | -5220   |
| 28    | -90   |
| 29    | 0   |

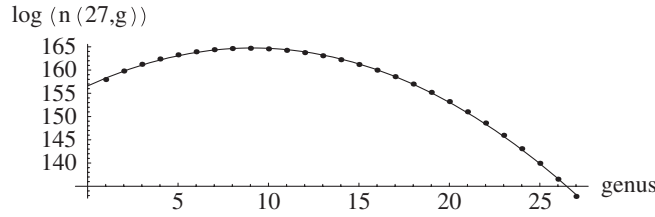


FIG. 10. The binomials dominate the behavior of large  $d$  Gopakumar-Vafa invariants. For the degree 27 class on the bicubic we find  $n_{27}^g \sim e^{167.747} e^{-0.0985(g-9.108)^2}$ .

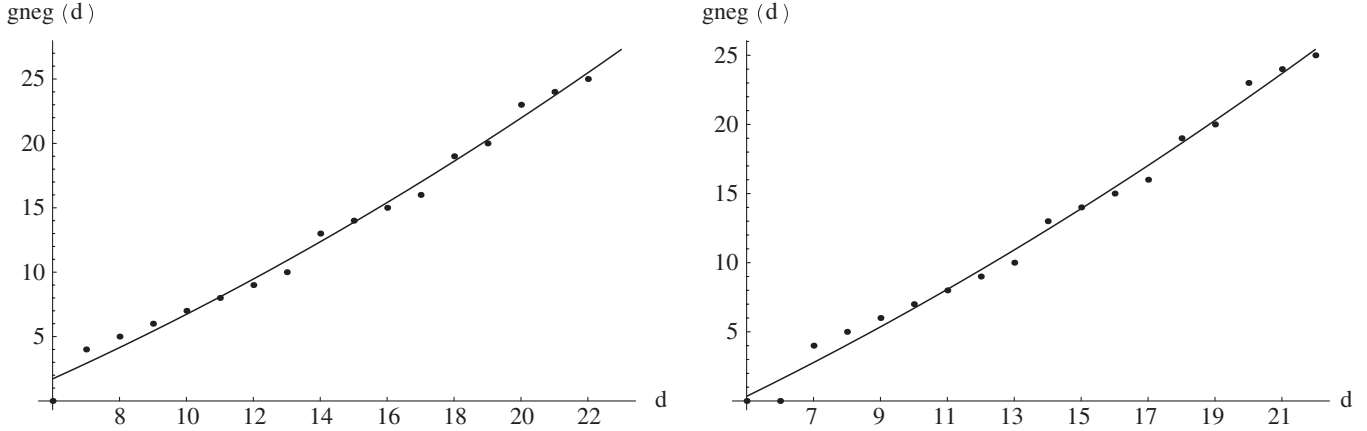


FIG. 11. The first occurrence of negative  $n_d^g$  for the quintic (on the right) and the bicubic (on the left). The fit is  $m(d) = a + bd + cd^2$  with  $a = -4.6$ ,  $b = .94$ , and  $c = .019$  as well as  $a = -5.2$ ,  $b = 1.0$ , and  $c = .017$  for these two, respectively.

to describe some of these general features. Typical data for high degree look as in Table VII.

The last nonzero entry from the smooth genus 28 complete intersection curve<sup>5</sup> (1, 2, 3, 3) of degree 18. By Castelnuovo’s theory  $\tilde{g} = 28$  is the largest possible genus for degree 18. The degree one constraint parametrizes a  $\mathbb{P}^5$ . The moduli space  $\mathcal{M}_{18}^{28}$  is a fibration of this  $\mathbb{P}^5$  over a projectivization of the 15 parameters in the quadratic constraint. I.e.  $\mathcal{M}_{18}^{28}$  is the total space of  $\mathbb{P}^5 \rightarrow \mathbb{P}^{14}$ , with Euler number  $\chi(\mathcal{M}_{d=18}^{g=28}) = 5 \times 15 = 90$  and  $n_{18}^{28} = (-1)^{5+14}90 = -90$ .

As it can further be seen in Table VII, the numbers grow from genus  $g = 0$  to  $g = 3$  and fall thereafter. This feature might be related to the binomials in the description of the moduli of space as a singular fibration of the Jacobian  $\text{Jac}_{28}$  of the  $g = 28$  curve over  $\mathcal{M}_{18}^{28}$ . In this description the contribution of a  $g = \tilde{g} - \delta$  curve comes from degenerating the genus 28 curve with  $\delta$  nodes. As explained in [4] the contribution of the degenerate Jacobians can be expressed by the Euler numbers of relative Hilbert schemes  $\mathcal{C}^{(n)}$  as

$$n_d^{\tilde{g}-\delta} = (-1)^{\dim(\mathcal{M})+\delta} \sum_{p=0}^{\delta} b(\tilde{g} - p, \delta - p) \chi(\mathcal{C}^{(n)}), \quad (\text{A1})$$

<sup>5</sup>A complete intersection curve (1,  $n$ , 3, 3) with degree  $9n$  has in general genus  $\tilde{g} = \frac{1}{2}(1 + 3n)(2 + 3n)$ .

with

$$b(g, k) = \binom{2g - 2}{k}.$$

A simple Gauss approximation of binomials fits the behavior of the  $n_d^g$  for large  $d$  relatively well. We show this in Fig. 10 for the bicubic at degree 27. The numbers  $n_d^g$  are exact and in contrast to (A1) they count correctly all contributions from colliding nodes, all contributions from reducible curves, as well as contributions from smooth curves in the class  $d$  with genus  $\tilde{g} < \tilde{g}$ .

Very important for the cancellations in the asymptotic behavior of the Donaldson-Thomas invariants is the occurrence of negative numbers. While it is clear that such contributions can arise if the dimensions of the D-brane moduli space are odd, we do not understand *a priori* the remarkable pattern with which these signs occur. The first occurrence of negative signs at  $g_{\text{neg}}(d)$  is graphed for the quintic and the bicubic in Fig. 11. The data suggest that  $g_{\text{neg}}(d)$  follows a parabola similar to the Castelnuovo bound. From the first occurrence of the negative sign the  $n_d^g$  are alternating in sign for  $g \ll \tilde{g}$ . For  $g \sim \tilde{g}$  the behavior becomes more erratic. The Gauss approximation for the absolute values of the  $n_d^g$  and the sign pattern is very characteristic of the degeneracies of microstates of a large black hole. In contrast the absolute value of the  $n_d^g$  is falling and the signs are alternating with  $(-1)^g$  starting at  $g = 0$

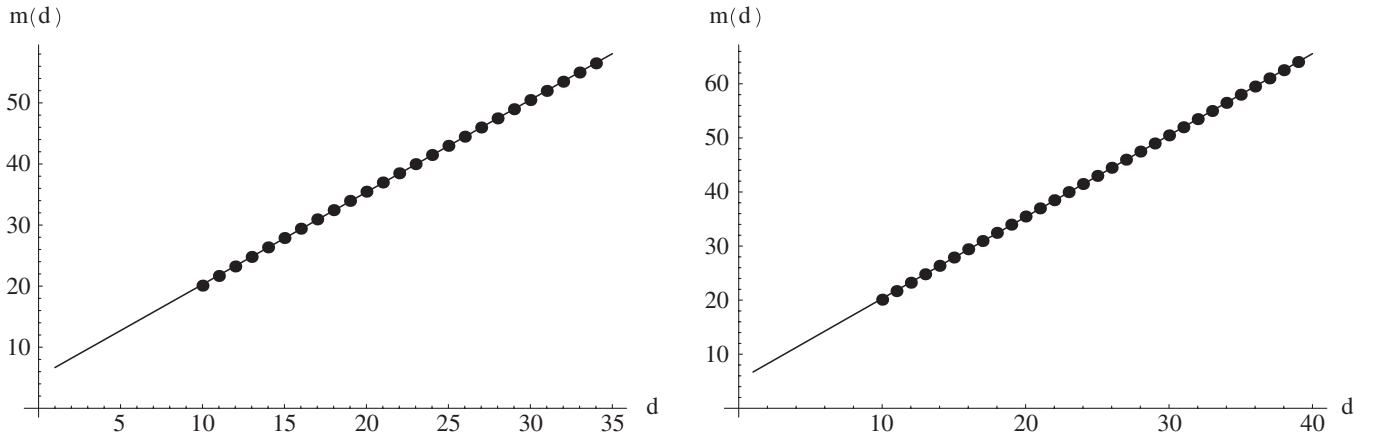


FIG. 12.  $m(d) = \log(M(d))^{3/4}$  for the quintic on the right and the bicubic on the left.  $a = 5.164$  and  $b = 1.511$  as well as  $a = 5.202$  and  $b = 1.509$  for the cases plotted.

for small black holes as shown, for example, for the ST model.

A further remarkable fact is the very universal scaling for the maximal value  $M(d)$  for  $n_d^g$  for given  $d$ . This value behaves like

$$M(d) = \exp((a + bd)^{4/3}) \quad (\text{A2})$$

with very similar values for  $a$  and  $b$  for different one-parameter models, as shown for the quintic and the bicubic in Fig. 12.

- 
- [1] A. Strominger and C. Vafa, Phys. Lett. B **379**, 99 (1996).  
 [2] J.R. David, G. Mandal, and S.R. Wadia, Phys. Rep. **369**, 549 (2002).  
 [3] R. Dijkgraaf, in *Classical and Quantum Black Holes*, edited by P. Fre *et al.* (Taylor & Francis, United Kingdom, 1999), p. 77.  
 [4] S. Katz, A. Klemm, and C. Vafa, Adv. Theor. Math. Phys. **3**, 1445 (1999).  
 [5] R. Gopakumar and C. Vafa, arXiv:hep-th/9809187; arXiv:hep-th/9812127.  
 [6] J.C. Breckenridge, R.C. Myers, A.W. Peet, and C. Vafa, Phys. Lett. B **391**, 93 (1997).  
 [7] M.x. Huang, A. Klemm, and S. Quackenbush, arXiv:hep-th/0612125.  
 [8] M. Bershadsky, S. Cecotti, H. Ooguri, and C. Vafa, Commun. Math. Phys. **165**, 311 (1994).  
 [9] S.H. Shenker, in *Random Surfaces and Quantum Gravity*, edited by O. Alvarez, E. Marinari, and P. Windey (Plenum, New York, 1992).  
 [10] M. Mariño, J. High Energy Phys. **03** (2008) 060.  
 [11] M. Guica and A. Strominger, arXiv:hep-th/0701011.  
 [12] F. Denef and G.W. Moore, arXiv:hep-th/0702146.  
 [13] H. Ooguri, A. Strominger, and C. Vafa, Phys. Rev. D **70**, 106007 (2004).  
 [14] I. Antoniadis, E. Gava, K.S. Narain, and T.R. Taylor, Nucl. Phys. **B455**, 109 (1995).  
 [15] T.W. Grimm, A. Klemm, M. Mariño, and M. Weiss, J. High Energy Phys. **08** (2007) 058.  
 [16] A. Klemm, M. Kreuzer, E. Riegler, and E. Scheidegger, J. High Energy Phys. **05** (2005) 023.  
 [17] A. Klemm and M. Mariño, Commun. Math. Phys. **280**, 27 (2008).  
 [18] M. Mariño and G.W. Moore, Nucl. Phys. **B543**, 592 (1999).  
 [19] A. Dabholkar, F. Denef, G.W. Moore, and B. Pioline, J. High Energy Phys. **10** (2005) 096.  
 [20] R. Dijkgraaf, J.M. Maldacena, G.W. Moore, and E.P. Verlinde, arXiv:hep-th/0005003.  
 [21] D. Gaiotto, A. Strominger, and X. Yin, J. High Energy Phys. **02** (2006) 024.  
 [22] S. Ferrara and R. Kallosh, Phys. Rev. D **54**, 1514 (1996).  
 [23] M. Guica, L. Huang, W. Li, and A. Strominger, J. High Energy Phys. **10** (2006) 036.  
 [24] R.M. Wald, Phys. Rev. D **48**, R3427 (1993).  
 [25] M. Alishahiha, J. High Energy Phys. **08** (2007) 094.  
 [26] A. Castro, J.L. Davis, P. Kraus, and F. Larsen, J. High Energy Phys. **04** (2007) 091; J. High Energy Phys. **06** (2007) 007.  
 [27] R. Dijkgraaf, G.W. Moore, E.P. Verlinde, and H.L. Verlinde, Commun. Math. Phys. **185**, 197 (1997).  
 [28] R. Dijkgraaf, E.P. Verlinde, and H.L. Verlinde, Nucl. Phys. **B484**, 543 (1997).  
 [29] S. Yamaguchi and S.T. Yau, J. High Energy Phys. **07** (2004) 047.  
 [30] <http://uw.physics.wisc.edu/~strings/aklemm/blackholedata/>.  
 [31] C. Vafa, Adv. Theor. Math. Phys. **2**, 207 (1998).  
 [32] C. Bender and S. Orszag, *Advanced Mathematical Methods for Scientists and Engineers* (McGraw-Hill, New York, 1978).

- [33] D. Maulik, N. Nekrasov, A. Okounkov, and R. Pandharipande, arXiv:math.AG/0312059.
- [34] S. Kachru and C. Vafa, Nucl. Phys. **B450**, 69 (1995).
- [35] A. Klemm, W. Lerche, and P. Mayr, Phys. Lett. B **357**, 313 (1995).
- [36] J. A. Harvey and G. W. Moore, Nucl. Phys. **B463**, 315 (1996).
- [37] K. Oguiso, Int. J. Math. **4**, 439 (1993).
- [38] T. Kawai, Phys. Lett. B **397**, 51 (1997).
- [39] S. Ferrara, J. A. Harvey, A. Strominger, and C. Vafa, Phys. Lett. B **361**, 59 (1995).
- [40] A. Dabholkar, N. Iizuka, A. Iqbal, and M. Shigemori, Phys. Rev. Lett. **96**, 071601 (2006).
- [41] I. Bena, D. E. Diaconescu, and B. Florea, J. High Energy Phys. 04 (2007) 045.
- [42] K. Bringmann and K. Ono, Inventiones Mathematicae **165**, 243 (2006).